INSTITUTO SUPERIOR TÉCNICO

PAPER FOR IIW MEETING, LJUBLJANA, SLOVENIA, 2001.
REF. XIII-1892/01

FATIGUE ANALYSIS OF WELDED JOINTS REHABILITATED BY HAMMER PEENING

By

Infante, V*., Branco*, C.M., Baptista, R.*

* ICEMS / IST, Avda. Rovisco Pais, 1049-001 Lisbon, Portugal

ABSTRACT

Fatigue strength has increased by a factor of 1.30 when the weld toe of T non loading carrying joints of St 52-3 carbon steel, loaded in bending, was treated by grinding or hammer peening. The hardness distributions and the microhardness have also shown that the depth of the zone affected by hammer peening is about 2.5mm, i.e. the material has hardened up to this depth. This was found to be the limit of the residual stress field created by the hammer peening.

The effect of hammer peening to repair or rehabilitate an as welded joint with fatigue crack of known depth was detailed, and equations were derived to quantify this effect. A fatigue life improvement factor, g, was defined for rehabilitation of joints by hammer peening. This factor was found to be dependent on the repair crack depth, increasing as the initial crack depth decreases, i.e. the treatment is more effective fore cracks with depths below 2mm, where the fatigue life of the repaired joint has increased by about one order of magnitude ($g \cong 10$).

A detailed life prediction analysis was carried out in the hammer peened specimens, where the effect of residual stresses induced by the treatment was analysed.

For joints that were subjected, initially, to a hammer peening treatment to increase their fatigue life in service, subsequent repair of fatigue cracks by hammer peening did not give any significant increase in fatigue life, as happens with those without the repair.

The residual stresses induced by hammer peening at the weld toe were found to be greater along longitudinal direction of the plate than along the transverse direction. The peak equivalent residual stresses near the weld toe were found to be of yield magnitude in compression, justifying the great benefit of hammer peening.

1. INTRODUCTION. BACKGROUND.

Today, due to economic constraints, the trend is to use the welded structures to the maximum of their life potential. To achieve this aim, considerable effort should be paid to inspection, monitoring and repair of the damaged zones. Life extension of ageing structures is possible to achieve without putting in danger the integrity of the structures, if rehabilitation methods are introduced. This project deals with the fatigue behaviour of welded joints in a structural steel subjected to the so-called "*local post-welding improvement techniques*", and is a follow-up of early research work carried out by the authors in this field (1, 2).

In this context, rehabilitation of the structure is achieved when the local treatment for repair gives a fatigue strength in the joint not below to the fatigue strength of the original detail before it was damaged. If the treatment is properly applied, the rehabilitation of the detail is assured, and the nature of the weld toe improvement methods can even produce a joint, after repair, with a fatigue strength and residual life higher than the initial detail, if this was not subjected to an improvement treatment. The repair treatment may arrest the original fatigue cracks, thus leading to infinite life or retard its growth.

Most of the life improvement techniques, as applied to original or new welds, were established in the 1960's and early 1970's ; they are summarised in early work available in references (3-5). A number of investigations have confirmed the benefit to be gained from improvement techniques, and large increases in the fatigue strength are usually obtained. In spite of this, some reluctance has been observed towards the introduction of improvement techniques into design recommendations, and only recently one method, toe grinding, has been allowed for in the design of offshore structures (6) and pressure vessels (7). TIG and plasma dressing can be even more effective than grinding (5, 8), but there is limited work to support this trend and, therefore, additional work is needed.

An analysis of an extensive amount of data available in the literature was made by Lieurade and co-workers (9). Four improvement techniques (*grinding, TIG dressing, hammer peening, shot peening*) for four joints (*butt, T joints, cruciform and longitudinal joints*) were taken into account in this study (9). The selected joints were those with thickness smaller than 25mm, loaded in air, with a stress ratio, R, between 0 and 0.1. Three classes of yield strength of base metal (YS<400, 400<YS<600. YS>600 MPa) were considered. All the S-N curves were above those of as-welded assemblies. The best results were obtained with hammer peening.

The rather large increase in the fatigue strength, due to the use of improvement techniques, can be explained by the significant increase of a so-called initiation phase, in addition to the crack propagation phase. During the initiation phase, the extension of existing "crack-like" defects is slowed down or even stopped. The duration of this phase increases with the local fatigue life (or the decrease in the stress range).

In a review recently presented by Maddox (10), the following conclusions and recommendations were defined for hammer peening:

- Sufficient passes are required to produce uniform indentation with smooth surface (four to six passes are adequate);
- A small diameter (<12mm) tool produces better coverage, but a larger diameter tool may need less passes. There is no unfavourable influence of poor weld profile on hammer peening in over-head position. The benefit of hammer peening was found to be reduced by prior compressive loading above 0.25 x yield. The fatigue S-N data justifies Class B design curve, with fatigue limit at $2x10^6$ cycles (better than burr grinding);
- The Class C is recommended with fatigue limit at $2x10^6$ cycles, to allow for variations in quality of the treatment. To allow for influence of mean stress, the Class C curve should be used with maximum applied tensile stress, if $R \geq 0$, or the full stress range, if $R \leq 0$.

The recommendations referred above are basically covered in the IIW specifications for weld toe improvement, which were used in the present work (11).

As referred above, improvement techniques can also be used to "rehabilitate" or repair welded structures where damage caused by fatigue, corrosion or other phenomena is detected in the weldment area. The damaged weld toes can be treated locally, and most frequently while the structure is in service. If the treatment is successfully applied, damage is quickly treated and, after the treatment, the initial undamaged mechanical properties can be restored or even improved, and a significant life extension period can be obtained. This will avoid the need for repair welding that would be the case if the detail had to be rewelded and set back into service again.

A report of significant fatigue life extensions in repaired welds by air-hammer peening is presented in (12). In another work by the same authors (13) it is shown that air-hammer peening of the local weld toe region is a practical and reliable technique for repairing welds with shallow surface cracks up to 3mm long. A claim is made that this technique has been used to repair fillet welds in bridges which have subsequently experienced more than a decade of heavy truck traffic without re-initiation. Cracks with depth greater than 3mm can be repaired by using rewelding procedures, but the results are sometimes contradictory (13). A review of the methods of repair is presented in (14), where emphasis is put on the fact that good results can only be obtained with local treatments by introduction of compressive residual stresses, hammer peening, shot peening, etc., if the depths of the existing crack are within the residual stress field created by the treatment. For this reason, only small cracks at the weld toe can be treated by these processes.

The more traditional fusion rewelding repair procedures are susceptible to induce metallurgical problems associated with the formation of brittle phases or other embrittling phenomena. Often, cracking occurs soon after rewelding in a material with different properties, difficult to evaluate. Hence, the risk of failure is greater with rewelding.

Results of an economical analysis on the effect of post-welding treatments of sound welds on the fatigue design of welded I beams are presented in (15). These results have shown significant cost savings for the different treatments and the maximum benefit was obtained with hammer peening. Additional work will continue in this area, also extensive to the cost effect on repaired welds.

The main technique used in this work relied on the introduction of compressive residual stresses peening (e.g. shot, needle, hammer) and spot-heating. In this case, the improvement technique does not necessarily reduces the stress concentration associated with the weld toe or remove the flaws. Instead, it has the effect of clamping the weld toe region in compression so that, under fatigue loading, the effective cyclic stress range is partly, or even completely, in compression and, hence, less damaging. Thus, the benefit is believed to be due to a reduction in the rate of growth of a fatigue crack from the weld toe discontinuity.

When these techniques are applied to a cracked weld where, usually, a fatigue crack exists, they are named *rehabilitation or repair techniques*.

Apart for the last point, there is a need to ensure that the benefit of a weld toe improvement technique seen in a laboratory test will be realised in a real structure. In this respect, it is known that differences in residual stress levels, fatigue loading conditions and environment can be significant.

With regard to the first two issues, there is evidence, from tests on welded steel beams, that improvement techniques, notably those relying on the introduction of compressive residual stresses, are less effective in large welded structures containing high tensile residual stresses, due to welding, than when they are used to treat small-scale specimens. This is undoubtedly linked to the fact that the increase in fatigue life, resulting for an improvement technique – particularly one relying in compressive residual stresses – tends to decrease with increase in applied tensile mean stress. Similarly, doubts exist about the effectiveness of improvement techniques, particularly those relying on compressive residual stresses, under variable amplitude loading, as normally occurs in real structures.

The results presented in this paper cover the effect of hammer peening, mainly as a repair technique, to rehabilitate fatigue crack joints at the weld toe, on the fatigue performance of non-loaded carrying cruciform joints loaded in bending in the main plate and made from a medium strength (class 400MPa yield) carbon steel. The hammer peening process is studied in detail, and results are presented on the impact forces distribution of residual stresses induced by the process, crack initiation and crack propagation data, morphology of treated surfaces and (or) cracks. The fatigue performance of the repaired detail is assessed with a herein defined gain factor.

2. EXPERIMENTAL DETAILS

2.1 MATERIAL AND SPECIMENS

Table I gives the composition and the nominal mechanical properties of the base and weld metal used in this study, a medium strength structural steel of the 400 MPa yield class (St 52-3, DIN 17100 specification), with a weld metal in a overmatching condition. The welds were made by the covered electrode process, and more details can be found in (16). The mechanical properties were also obtained at room temperature in tensile, compressive and LCF tests carried out in cylindrical specimens of 8-9mm diameter and 25mm gauge length machined from 12.5mm thick steel plates.

TABLE 1
CHEMICAL COMPOSITIONS AND NOMINAL MECHANICAL PROPERTIES OF THE BASE AND WELD METAL OF THE STEEL TESTED

Chemical Composition

Base Metal

Element and Content						
C	Si	Mn	Cr	Mo	Ni	Ti
0.131	0.413	1.44	0.063	0.024	0.034	0.009

Element and Content						
Al	V	Cu	Co	Nb	P	S
0.029	0.043	0.018	0.013	0.005	0.011	0.005

Weld Metal

Element and Content							
C	Si	Mn	Cr	Ni	Mo	P	S
0.08	0.45	1.28	0.50	1.87	0.37	0.017	0.01

A- Mechanical Properties

Base Metal

0.2% yield stress, σ_{ys}=410 MPa
Ultimate tensile stress, σ_{uts}=555 MPa
Rupture strain, ε_R=28%

Weld metal

σ_{UTS} = 770 MPa
0.2 yield stress = 690 MPa
Rupture strain, ε_R = 15%

The cyclic stress-strain curve of the material was obtained with one step level tests in twelve cylindrical specimens and under reversed cycling (R=-1 and, also, R=0 in tension and compression). The material has exhibited mainly cyclic strain hardening behaviour. Values of the strain hardening coefficient and exponent were obtained.

Figs. 1 shows the loading arrangement and the dimensions of the specimens.

Grinding of the weld toes was achieved with a set of abrasive barrel type carbide tools, rotating at high speed and pressed against the surface of the weld toe.

For hammer peening, a small portable pneumatic hammer was used (Fig. 2), fitted with a special hard metal tool, instrumented with four strain gauges bonded in full bridge (Fig. 2) to measure the impact forces and stresses during the hammer peening working cycles. The tool diameter was approximately 8.5mm, the air pressure was 3.5 bar and four passes, along the transverse direction of the specimen, were applied. The impact energy was approximately 11J, and the frequency 3000 blows/minute (bumps/minute).

2.2 Local Geometry at the Weld Toe

Both for the as welded and treated joints, the radius and angle at the weld toe were measured in the specimens using an X-Y table measuring facility, fitted with a video monitor optical system and capable of accuracies of 0.01mm and 0.5° for the radii and angles, respectively.

The results obtained in the analysis of these data were statistically treated, and the relevant data may be found in (16).

2.3 Fatigue Tests

The fatigue tests were carried out under constant amplitude loading in a $\pm$ 250 kN capacity servohydraulic fatigue test machine, with the testing arrangement illustrated in Fig. 1. The frequency was 10-15 Hz, and the stress ratio, R=0.1. The bulk of the tests was carried out until complete failure of the specimen or up to a number of cycles close to 6.0×10^6, time when the fatigue test was stopped.

In the majority of the specimens, including all the cracked ones subjected to rehabilitation, six strain gauges were bonded very close to the weld toes of the attachment, as shown in Fig. 3. These strain gauges measured the variation of the local strain at the weld toe and along the width of the specimen, caused by the initiation and propagation of the fatigue cracks at the weld toe through the thickness direction of the longitudinal plate. The strain data was used to establish the onset of fatigue crack tip marking and to define the crack geometry to be repaired, afterwards, by hammer peening.

Misalignment was checked in some specimens, using strain gauges, and it was found to be negligible.

2.4 Hardness Measurements

Vickers micro hardness data with 1Kg and 25gf loads were obtained along the longitudinal directions of the plate, close to the upper and lower surfaces. The variation of hardness along the thickness of the specimen at the weld toe and in the crack propagation direction was also obtained, with loads of 0.025Kgf (25 grams) and 1Kgf. The main objective of these tests was to compare the hardness distributions for the as welded and hammer peened specimens. Calibration curves of HV1 and HV0.025Kgf microhardness against true stress and true strain measured in tensile tests were also obtained to compare with the stress strain curves of the specimens of the base metal and to derive a stress strain curve valid for the weld metal.

3. RESULTS AND DISCUSSION

3.1 Analysis of the Hammer Peening Process

The variation of the hammer peening impact forces and stresses in the tool, as measured by the strain gauges, is depicted in Fig. 4. The duration of the treatment (working cycle) was about 6s. The peak stress and force in the tool were, respectively, -27.70 MPa and -3136.5N. The mean, or equivalent, stress and force gave, respectively, the values -12.0 MPa and 1359N. These mean values are the static values who produce the same area under the dynamic stress or load cycle imposed by the tool in the material (Fig. 4). These values of the force measured in the hammer peening working cycle (Fig. 4) were used later in the work in the numerical simulation of the process, to compute the residual stresses and strains at the weld toe area, generated by the treatment.

3.2 Hardness Data

The hardness profiles HV1 along the thickness direction, y, of the plate, along a line passing through the weld toe (crack propagation direction), are plotted in Fig. 5a) for the as welded joints, and Fig. 6b) for the hammer peened joints. In both cases, there is an increase of hardness approaching the plate surface at the weld toe in the HAZ. In the as welded joints, the thickness of the HAZ in the thickness direction is close to 4mm (Fig. 5a)), as equally confirmed by the macro in Fig. 1 a). In the hammer peened joints, an increase in hardness was obtained, and the hardness profile shows peak hardness values close to 260 HV1 near the surface at the weld toe zone (Fig. 5b)). Fig. 5b) also shows that the depth of the zone affected by the hammer peening is about 2.5mm, i.e. the material has hardened up to this depth, and this should be the limit of the residual stress field created by the hammer peening. This result also indicates that the treatment could be effective if the crack is inside this hardened zone, where the hardness increases from near the value 180 HV1 of the base metal up to near 260 HV1 at the surface at the weld toe.

The plot of the perlite microhardness for the load of 25gf is shown in Fig. 6), and confirms the data shown in Figs 5 a), b), i.e. the steepest gradient of the hardness values occurs up to a depth of approximately 4mm. In the most affected zone (up to a depth of near 4.0mm), the hardness varies between 320 and 280HV (Fig. 6).

As expected, the perlite microhardness is higher than the 1Kgf hardness, since both perlite and ferrite grains are indented with the higher load.

The microstructures of the base metal, weld metal and HAZ are also shown. The steel presents the typical perlite-ferritic microstructure, with an average grain size of 20μm. Grain refinement can be seen in the HAZ.

3.3 Monotonic and Fatigue Data in Plain Specimens

The test programme included a series of tests aimed to characterise the monotonic and cyclic behaviour of the base metal under tensile and compressive loads. Data under compressive loading was needed to model the compressive effect of the hammer peening process and to compare with tensile data. The tests were:

- monotonic in tension, up to failure, to obtain the stress strain curves (nominal and true);
- similar in compression, up to the point of buckling;
- LCF in tension-compression under reversed cycling for R=-1
- LCF in tension only under pulsating tension (load cycling) with R=0;
- LCF in compression only under pulsating compression (load cycling) with R=0.

The strength and ductility parameters for these tests are given in Table 2, and those include Young's modulus, strain hardening exponent and coefficient, uniform elongation. Fracture ductility, ε_R, yield stress (0.2%), ultimate tensile stress, fracture stress and the correlation coefficients, r^2, of the Ramberg-Osgood relationships.

In Table 2, $\sigma_{0.2}$ and $\varepsilon_{0.2}$ are the nominal stress and strain for the 0.2% offset plastic strain under monotonic loading, E is the Young's modulus, σ_{UTS} the ultimate tensile or compressive strength, σ_f the fracture stress and K' and n' refers to the cyclic stress-strain curve (strain cycling, equation (1)).

TABLE 2 – MONOTONIC AND CYCLIC STRESS STRAIN DATA

A – Tension

$\sigma_{0.2}$ (MPa)	$\varepsilon_{0.2}$ (%)	E (MPa)	σ_{UTS} (MPa)	σ_f (MPa)	ε_R (%)	K'	n'	r^2	
415.3	0.56	200302	571.2	356.5	14.27	-----	-----	-----	
406.9	0.50	218254	569.4	358.3	15.04	-----	-----	-----	
411.1	0.53	214273	567.3	357.4	14.65	1015.31	0.1535	0.966	Mean

B – Compression

$\sigma_{0.2}$ (MPa)	$\varepsilon_{0.2}$ (%)	E (MPa)	σ_{UTS} (MPa)	σ_f (MPa)	ε_R (%)	K'	n'	r^2	
420.4	0.27	205949	696.5	696.5	12.77	-----	-----	-----	
416.9	0.31	203625	638.0	638.0	7.92	-----	-----	-----	
418.7	0.29	204787	667.3	667.3	10.35	1015.31	0.1535	0.966	Mean
Limited by buckling and (or) non uniform compression									

The equation of the cyclic curve in tension was:

$$\frac{\Delta\sigma}{2} = 1130.32\left(\frac{\Delta\varepsilon_p}{2}\right)^{0.1707} \qquad (1)$$

where $\Delta\varepsilon_p$ is the plastic strain amplitude (width of the hysteresis loop for $\Delta\sigma$=0)-

The cyclic stress-strain curves in tension and compression under load control with R=0 were obtained. In both cases, rachetning or cyclic creep accumulation was observed until close to failure, and empirical correlations of the accumulated cyclic plastic strain, $\Delta\varepsilon$, against the number of cycles were obtained, but not used in the analysis. The data shows that the accumulated plastic strain in tension is higher than in compression. In compression, it appears that a saturation level of ε_{cc}=0.09 is reached, where strain does not increase with the number of load applications and, hence, a shakedown condition in compression is reached.

The fatigue life data for strain cycling with R=-1 is given in Table 3. The Coffin-Manson equation gave:

$$\frac{\Delta\varepsilon_p}{2} = 0.3574(2Ni)^{-0.0856} \qquad (2)$$

with a correlation coefficient of r^2=0.966.

TABLE 3
FATIGUE LIFE DATA FOR STRAIN CYCLING R=-1. STEEL ST 52-3

Test Number	$\Delta\sigma$ (MPa)	$\Delta\varepsilon_t$	$\Delta\varepsilon_e$	$\Delta\varepsilon_p$	Nº cycles N_r	Nº reversions $2N_r$
1	490.4	0.01005	0.002305	0.007745	965	1930
2	464.9	0.00814	0.002185	0.005955	1463	2926
3	442.2	0.00616	0.002078	0.004082	1700	3400
4	421.7	0.00510	0.001982	0.003118	3840	7680
5	399.0	0.00413	0.001875	0.002255	4283	8566
6	355.5	0.00302	0.001671	0.001349	12800	25600
7	542.9	0.01505	0.002551	0.001249	190	380
8	523.7	0.01254	0.002461	0.010079	377	754
9	335.0	.000241	0.001574	0.000836	33220	66440
10	331.3	0.00211	0.001557	0.000553	30000	60000
11	330.4	0.00242	0.001553	0.000867	16800	33600
1	485.4	0.00976	0.00228	0.00772	363	726
2	549.1	0.02943	0.00258	0.02708	57	114
3	536.1	0.01952	0.00252	0.01734	74	148
4	499.4	0.00976	0.00235	0.00774	330	660
5	514.7	0.01947	0.00242	0.01737	138	276

The Basquin equation for the elastic strain components is:

$$\frac{\Delta\varepsilon_e}{2} = \frac{869.1}{E}(2Ni)^{-0.0856} \tag{3}$$

with a correlation coefficient of r^2=0.94.

Monotonic stress-strain curves were also derived from microhardness data obtained in the tensile tests. The objectives of these tests were to compare the results with the $\sigma\varepsilon$ curve obtained from tensile testing, and to use the data to predict a stress-strain curve also valid for the weld metal and HAZ, zones where testing is not possible to carry out.

In Fig. 7a), b) the variation of Vickers hardness, HV1, with rue stress, σ (Fig. 7a)) and true strain, ε (Fig. 7b)), are presented. These results were obtained in tensile tests in two cylindrical specimens of base metal with ϕ=8mm diameter (the same geometry of the LCF specimens, subjected to incremental loading up to the maximum load. The hardness was measured in the specimen after unloadings from the values of σ, ε plotted in Figs. 7a), b). Non linear relationships were obtained, and the equations and the correlation coefficients are given in Fig. 7.

From the data in Fig. 7a), b) the resulting true stress-true strain curve was obtained, and is shown in Fig. 7c). This curve was assumed as the constitutive equation of the weld metal and HAZ in the range of hardness shown in Fig. 5a) up to the depth of 4mm (180<HV1<230). Note that, in this case, there is no trend of variation in hardness from the weld metal to the HAZ, due to the overmatch condition of the weld metal (see Table 1). A very good agreement was obtained between the stress-strain curve of Fig, 7c), derived form hardness measurements, and the nominal values for the material referred in Table 1.

3.4 Fatigue Data in the Welded Joints

The set of S-N data is given in Table 4, and typical macros of the fracture surfaces of some fatigue specimens are shown in Fig. 8a) to c).

Fig. 8a) refers to as welded specimens without any improvement or repair treatment applied. Fatigue marking was carried out in Fig. 8a). Figs. 8b), c) are for hammer peened specimens. Marking was done to verify the crack growth rate model and check the sensitivity of the strain gauge technique to relate the variation of local strain with the crack length and depth. Marking was carried out after a variation of local strain between 10 to 40% was detected, which occurred for cracks sufficiently great to be easily inspected. The number of cycles for marking was 10000 to 15000 cycles with R=0.5.

The second example macro (Fig. 8b)) is from one of the specimens (Ref. 57), where the repair treatment produced the greatest benefit in terms of fatigue life increase. In this specimen, hammer peening was applied to a weld toe crack of a=1.27mm, well inside the depth of the region affected by the treatment (Fig. 5). Mainly due to this reason, a new or secondary cracking initiated also from the crack tip region of the initial crack, which causes retardation in the cracking process.

In all of the repaired specimens fatigue marking was carried out, as referred above, to get a better definition of the fracture surface. Figs. 8c) is an example of repaired joint by hammer peening, where hammer peening was also applied after welding as an improvement technique. In Fig. 8c) the repaired crack was longer than in Fig. 8b).

The morphology of the fracture surfaces of the repaired cracks was analysed with the SEM, both at the surface of the specimen and on the vicinity of the crack tip treated by hammer peening. The objectives of these observations were to compare the cracking nodes and analyse the effect of the plastic deformation. Some of the more relevant images are shown in Fig. 9a), b), c). Thus, Fig. 9a) is the near surface region at the weld toe of an hammer peened specimen which was continuously tested up to failure. The grain structure shows signs of extensive plastic deformation. The main failure mode is mixed, with ductile striations growing in a severely deformed zone, where secondary cracking is also visible and microvoid coalescence facilitated by the ductile stress-strain field.

The second example (Fig. 9b))shows the crack profile of a repaired crack with a=1.441mm. The area of the crack was treated by hammer peening. The fracture surface shows the plastically deformed crack surfaces of the original crack.

The fracture surfaces in Figs. 9b), c) are for two specimens tested at the same nominal stress value of 400MPa, but with cracks of different depth repaired by hammer peening. After the treatment, the test continued, and a second crack initiated in the first cracked zone.

The second "repaired crack" with a>1.441mm has propagated by a ductile striation mechanism, accompanied by ductile void formation. A similar mechanism as in Fig. 9b) was observed for a longer crack of a=4.0mm, as shown in Fig. 9c). In this case, the extent of plastic blunting at the treated crack surfaces is higher due to the higher value of the range of the stress intensity factor and the associated higher value of CTOD (Fig. 9c)).

The variation with the number of cycles of the local strain at the weld toe, was measured with the strain gauges at the weld toe. Usually, fatigue cracks have initiated in this location.

TABLE 4 – S-N DATA OBTAINED IN THE FATIGUE TESTS. T JOINTS. BENDING. R≅0. MEDIUM STRENGTH ST 52.3 STEEL.

Ref.	$\Delta\sigma$ [MPa]	N_i [Cycles]	N_r [Cycles]	Condition
1	342.8	-	293674	As welded only
10	475	-	50239	As welded only
11	475	-	52338	As welded only
14	450	-	57053	As welded only
15	450	-	53801	As welded only
21	350	-	411151	As welded only
25	400	-	128068	As welded only
30	275	-	5020162	As welded only
31	275	-	5000000	As welded only
44	400	-	249688	As welded only
45	400	-	112243	As welded only
2	345.5	-	3193530	Toe ground only
3	400	-	920023	Toe ground only
5	450	-	819619	Toe ground only
6	450	-	1309062	Toe ground only
7	450	-	716693	Toe ground only
8	400	-	2299608	Toe ground only
12	350	-	5000000	Toe ground only
13	350	-	3893059	Toe ground only
16	300	-	10917187	Toe ground only
49	500	-	57532	Toe ground only
50	500	-	72134	Toe ground only
51	400	-	124220	Toe ground only
52	400	-	143041	Toe ground only
17	500	-	140219	Hammer peening only
18	500	-	82762	Hammer peening only
19	400	-	640525	Hammer peening only
20	400	-	1107785	Hammer peening only
32	375	-	8488522	Hammer peening only
33	375	-	8253048	Hammer peening only
34	525	-	120446	Hammer peening only
35	525	-	223868	Hammer peening only
36	550	-	60280	Hammer peening only
37	550	-	29094	Hammer peening only
39	400	-	325850	Hammer peening only
40	550	-	30299	Hammer peening only
41	400	-	305815	Hammer peening only
43	500	-	66547	Hammer peening only
48	385	-	731761	Hammer peening only
55	525	-	36931	Hammer peening only (7 bar)
56	400	-	331888	Hammer peening only (7 bar)

TABLE 4 (CONT.) – S-N DATA OBTAINED IN THE FATIGUE TESTS. T JOINTS. BENDING. R≅0. MEDIUM STRENGTH ST 52.3 STEEL.

Ref.	$\Delta\sigma$ [MPa]	N_i [Cycles]	N_r [Cycles]	Condition
22	325	1357537	2024529	As welded only with fatigue marking
23	325	260000	489201	As welded only with fatigue marking
24	325	65100	1398259	As welded initially and crack repaired by hammer peening
26	400	75000	156255	As welded initially and crack repaired by hammer peening
27	400	10000	230613	As welded initially and crack repaired by hammer peening
28	400	100000	379581	As welded initially and crack repaired by hammer peening
29	300	2080000	3401893	As welded initially and crack repaired by hammer peening
53	400	100000 261254 *	543810	As welded initially and crack repaired by hammer peening
54	325	360000	514619	As welded initially and crack repaired by hammer peening
57	325	470000 263809 *	3506191	As welded initially and crack repaired by hammer peening
57	400	-	900266	As welded initially and crack repaired by hammer peening
38	500	10000	111939	Hammer peening initially and crack repaired by hammer peening
46	500	85000	144252	Hammer peening initially and crack repaired by hammer peening
47	500	30000	93809	Hammer peening initially and crack repaired by hammer peening

*N_{iaH} – Nº of cycles of crack initiation after hammer peening

No meaningful correlation was obtained between the strain variation at the weld toe, induced by fatigue cracking and other parameters such as crack length, nominal stress or fatigue life. This is mainly due to the fact that, with the small number of strain gauges bonded at the weld toe, there is a small probability to have a strain gauge in the zone where fatigue cracks have initiated. However, a general trend was to obtain crack lengths greater than 2.0mm for strain variations greater than 25% from the initial value.

In Table 4, N_i is the experimentally obtained number of cycles of crack initiation from the start of the test. This value was defined as the number of cycles where the first variation (usually reduction) of strain was detected in the strain gauges at the weld toe. These values are indicated in the graphs of Fig. 10. N_r is the total number of cycles to failure, including the repair or rehabilitation treatment, as appropriate.

In some specimens, loss of strain was observed in the zone of crack initiation, while, in others, the local strain increased at the onset of crack propagation (Fig. 10b)). This depended on the distribution of bending stress at the weld toe region.

In the specimen of Fig. 10a) (an as welded specimen), 10000 cycles of marking were applied at R=0.5after a strain reduction of 40% from the N_i point. In the specimen of Fig. 10b) marking was also carried out, but hammer peening was applied immediately. The criteria to initiate the marking was 15% strain increase.

The S-N curves of the non-repaired T joints are plotted in Fig. 11. The equations obtained for the mean regression lines for 50% probability of failure, assuming N_i as the dependent variable, are given in Table 5, next. The gains in fatigue strength for $2x10^6$ and $3x10^6$ cycles were also calculated.

TABLE 5 – PARAMETERS OF THE S-N CURVES IN FIG. 22. 3PB. T JOINTS. NON-LOAD CARRYING. ST 52-3 STEEL.

Ref. (R=0.1)	m	K_0	r^2	Gain in fatigue strength at $2x10^6$ cycles	Gain in fatigue strength at $3x10^6$ cycles
As welded	8.263	4.99E+26	0.9469	1	1
Ground	11.068	4.93E+34	0.9380	(367.4/294.0)=1.25	(350.0/294.0)=1.19
Hammer Peened	6.751	1.85E+23	0.7866	(325.6/294.0=1.11)	(375.0/294.0)=1.27

An improvement in fatigue behaviour was obtained in the treated joints. Thus, for fatigue lives above 10^6 cycles (Fig. 11), hammer peening provides higher fatigue strength since higher fatigue limit stresses were obtained (≅ 350 MPa). Progressively higher fatigue crack initiation periods were obtained in the toe ground and hammer peened joints, as reflected by the higher values of m in the equation of the S-N curve (Table 5). Some results, obtained with a 7 bar hammer peening pressure, are also included for comparison, and these show that there is no significant variation in the fatigue strength of the joint when the pressure is increased from 3.5 to 7.0 bar.

The results show that the fatigue strength of this detail is very high. Comparisons can be made with available fatigue design S-N codes (17, 18), and recommendations will be proposed to take into account the effect of these treatments on the fatigue design curves.

Since experimental data was available to define both, the crack initiation period and the crack propagation from the first induced crack at the weld toe, to be treated by hammer peening, a study was made on predictive techniques to quantify these periods. Thus, a fracture mechanics prediction was carried out using Paris law relationships obtained previously in this and other steels, similar in what concerns the composition and the mechanical properties (19, 20). The selected values for the constant C and exponent, m, were

Weld metal: $C=4.02\text{x}10^{-9}$mm/cycle; m=2.48

Base metal: $C=1.36\text{x}10^{-11}$mm/cycle; m=3.34

Table 6 a), b) gives the results of the predictions, as well as the experimental results obtained in the tests in the instrumented as welded specimens which were not repaired. The predictions were carried out using a previously derived crack propagation program, already tested successfully in other welded geometries (21, 22). The formulations of the PD6493 document (23) were used for the stress intensity factor equations.

Crack growth was analysed in two stages, from an initial defect value a_0 up to the crack marking depth (e.g. Fig. 10), and from crack marking up to the final crack depth of B/2. It was assumed that the shape of the propagating crack was such that a/2c=constant from a_o up to a_f. It should be pointed out that the shape of the marking crack was not estimated with high accuracy, due to experimental difficulties.

Other criteria to define N_i can be defined such as the number of cycles for 5 or 10% strain variation from the initial value (24).

$$N_{Te} = N_i + N_{bm} + N_{am} \tag{4}$$

In Table 6,

N_i – cycles for the first measurable crack initiation, as detected by the first variation in strain (Fig. 10) of the strain gauges placed at the weld toe (Fig. 3);

a_o, c_o – average depth and semi-surface length of the initial measured crack;

a_m, c_m –average depth and semi-surface length of the crack at the marking;

N_{bm} – experimental number of crack propagation cycles before marking (Fig. 10);

N_{am} –experimental number of crack propagation cycles after marking, up to a_f=B/2≅6.25mm;

N_{bmp}, N_{amp} –Similar as N_{bm} and N_{am}, but predicted by the program (21, 23);

N_{Te}, N_{Tp} – total experimental (initiation + propagation) (Fig. 10) and predicted number of cycles of crack propagation, N_{Tp}, for the as welded specimen.

TABLE 6 – EXPERIMENTAL AND PREDICTED VALUES OF FATIGUE LIFE FOR THE 3PB INSTRUMENTED AS WELDED NON REPAIRED SPECIMENS. R=0.1. ST 52-3 STEEL.

Spec	a_o (mm)	c_o (mm)	a_m (mm)	c_m (mm)	N_{bm} (1)	N_{bmp} (2)	Ratio (1/2)
22	0.1	0.912	1.67	15.224	310000	356992	0.87
23	0.1	0.698	3.862	26.947	123600	105601	1.17

Spec	N_{am} (3)	N_{amp} (4)	Ratio (3/4)	N_i (5)	N_{Te} (6)	N_{Tp}	Ratio (5/6)
22	356992	59230	6.03	1357537	2024529	416222	0.67
23	105601	18665	5.66	260000	489201	124266	0.53

$$N_{Tp} = N_{amp} + N_{bmp} \tag{5}$$

The results show good agreement between the experimental and the predicted number of cycles of crack propagation up to marking, i.e. when the crack is basically growing in the weld metal affected area. For crack lengths greater than the marking crack (a_m, c_m) the experimental values N_{am} are higher than the predicted N_{amp}, which could be attributed to variations in microstructure and also inaccuracies in the measurement of the marking crack.

In these as welded specimens, nearly 50% of the total fatigue life is spent in crack initiation up to a measurable size or event (ratio 5/6 in Table 6).

Similar results as in Table 6, but for the specimens repaired by hammer peening are given in Table 7. Table 7a) gives an assessment of the effect of hammer peening, and Table 7b) gives the experimental results obtained on the cracked specimens repaired by hammer peening, together with the predicted values given by the program.

In these tables, the meaning of the variables is:

a_H, c_H – average depth and semi-surface length of the crack repaired by hammer peening (after marking);

N_{bH} – experimental number of cycles of crack propagation before hammer peening (a_H, c_H) (after N_I and including the number of cycles of marking);

N_{aH}– experimental number of cycles after hammer peening (initiation, N_{iaH} (N'_{iaH})+ propagation, N_{paH} (N'_{paH}));

N_{bHp}, N_{aHp} – similar as N_{bH} and N_{aH}, but the number of cycles of crack propagation predicted by the program;

N_{Te} – total experimental number of cycles;

N_{paH} – experimental number of cycles of crack propagation after hammer peening;

N'_{paH} – predicted number of cycles of crack propagation after hammer peening;

N_{iaH}, N'_{iaH} – number of cycles of crack initiation after hammer peening (respectively for N_{paH} or N'_{paH});

N_{Tp} – total predicted number of cycles of crack propagation, plus N_i.

For these results, in Table 7 a), b), , the following equations apply:

$$N_{Tp} = N_{bHp} + N_{aHp} + N_i \quad (6)$$

$$N_{Te} = N_i + N_{bH} + N_{aH} \quad (7)$$

$$N_{aH} = N_{iaH} + N_{paH} \quad (8a)$$

$$N'_{aH} = N'_{iaH} + N'_{paH} \quad (8b)$$

where N_i is the number of cycles for crack initiation before hammer peening, obtained experimentally (e.g. Fig. 10b)).

TABLE 7 – A) EXPERIMENTAL AND PREDICTED VALUES OF THE FATIGUE LIVES OF THE REPAIRED JOINTS. 3PB WELDED JOINTS. ST S2-3 STEEL. R≅0.1.

Spec.	a_o (mm)	c_o (mm)	a_H (mm)	c_H (mm)	N_{bH} (1)	N_{bHp} (2)
24	0.1	0.222	2.413	5.357	202306	217984
26	0.1	0.575	3.18	18.292	42321	42485
27	0.1	0.271	2.50	7.717	88458	105845
28	0.1	0.230	4	9.2095	109237	146011
29	0.1	0.176	3.3	5.8065	427107	414060
53	0.1	0.829	1.441	11.959	38746	24692
54	0.1	0.440	6.1	26.84	132775	128572
57 (325MPa)	0.1	0.278	1.27	3.688	36191	141597
57 (400MPa)	0.1	0.278	1.27	3.688		

TABLE 7A) – CONT.

Spec.	Ratio (1/2)	N_{aH} (3)	N_{iaH} or N'_{iaH}	N_{paH} (4)	N'_{paH} (5)	Ratio (3/5)	Ratio (4/5)
24	0.93	1130853	1053861	---	76992	14.69	---
26	1.00	38934	31732	---	7202	5.41	---
27	0.84	132155	103872	---	28283	4.67	---
28	0.75	170344	148786	---	21558	7.90	---
29	1.03	894786	798018	---	96768	9.25	---
53	1.57	405064	261254	143810	8407	48.18	17.11
54	1.03	21844	21259	---	585	37.34	---
57 (325MPa)	0.25	6000000	5911757	---	88243	67.99	---
57 (400MPa)		394075	263809	130266	52738	7.47	2.47

In the first stage of cracking (before hammer peening), good agreement was also obtained between the experimental and predicted values of the number of cycles of crack propagation (N_{bH}/N_{bHp})

All the data in Table 7 was obtained in strain gauged specimens (Fig. 3). In specimens 53 and 57, strain gauges were also bonded at the weld toe after hammer peening of the induced crack. Hence, only in these three specimens only in these specimens, the number of cycles for crack initiation and crack propagation after hammer peening can be separated. The criteria for the definition of N_{iaH} was the same as for N_I, before repair, i.e. N_{iaH} is the number of cycles detected at the onset of variation of strain range, measured in the strain gauges at the weld toe, after hammer peening.

The results in Table 7 give very long crack initiation periods in the repaired cracks by hammer peening, as can be seen from the ratio N_{aH}/N'_{paH}, who varies between 4.67 and 67.99. The ratio between the estimated number of cycles of crack propagation after hammer peening, N_{paH}, and the predicted one given by the fatigue life program N'_{paH}, is also great, and this will be discussed next.

Table 7b) summarises the results obtained in the repaired joints, and the S-N data is plotted in Fig 12. The results show that this rehabilitation by hammer peening has increased the fatigue strength, since all the data lies above the line for the as welded joints. However, the fatigue strength of these damaged hammer peened specimens is less than the fatigue strength of the initially undamaged hammer peened specimens (Fig. 11). The values of the ratio N_I / N_{Te} show that the number of cycles for the initiation of the crack before repair is considerably smaller than the total fatigue life of the rehabilitated joint. The number of cycles after hammer peening of the damaged crack, N_{aH}, covers a significant proportion of the total fatigue life, N_{Te} (N_{aH}/N_{Te} data in Table 7b)). The predicted life in crack propagation of the damaged hammer peening joints, N_{Tp}, is considerably smaller than the total fatigue life of these joints, due to significant increase of the crack initiation phase, N_{iaH}, induced by the repair by hammer peening (Table 7b)).

In these specimens, the geometry of the repaired crack was more clearly defined than in the as welded specimens. Hence, very good agreement was found between N_{bH} and N_{bHp} (Table 7a)).

TABLE 7 – COMPARISON OF FATIGUE LIVES OF THE SPECIMENS IN TABLE 7A).

Spec.	N_i (1)	N_{aH} (2)	N_{Te} (3) N_{Tp} (4)	Ratio (1/3)	Ratio (2/3)	Ratio (3/4)	N_{ebh} (5)	Ratio g (3)/(5)
24	65100	1130853	1398259 360076	0.05	0.81	3.88	344398	4.06
26	75000	38934	156255 124687	0.48	0.25	1.25	124523	1.25
27	10000	132155	230613 144128	0.04	0.57	1.60	126741	1.82
28	100000	170344	379581 267569	0.26	0.45	1.42	230795	1.64
29	208000 0	894786	3401893 2590829	0.61	0.26	1.31	2603875	1.31
53	100000	405064	543810 133099	0.18	0.74	4.09	147153	3.70
54	360000	21844	514619 489157	0.70	0.04	1.05	493360	1.04
57 (325MPa)	470000	>6000000	6506191 231826	0.07	0.92	28.06	594434	10.95
57 (400MPa)		394075	900266 138548		0.44	6.50		

The predicted results in Table 6 were obtained using the values of C and m for the weld metal, as justified by Fig. 1. For the analysis of crack propagation after marking and after hammer peening (Table 4), the values of C and m assumed were those for the base metal, since for the size of these repaired cracks, crack tip is essentially in the base metal. Hence, the effect of the residual stress field was not analysed. Results of the work, taking into account the residual stress field induced by the hammer peening treatment, are presented later in the paper. This latter effect is the main factor to explain the large difference found between the values of N_{paH} and N'_{paH} ($N_{paH} > N'_{paH}$), since N'_{paH} does not consider the beneficial effect of the compressive residual stress field, reducing the crack speed.

The gains in fatigue life due to treatment, g, can be given by the relation:

$$g = \frac{N_{Te}}{N_{ebh}} \tag{9}$$

Where g is the rehabilitation ratio and N_{ebh} would be the expected life of the joint (Table 7), without the repair, given by the relation

$$N_{ebh} = N_i + N_{bH} + N'_{paH} \tag{10}$$

where N'_{paH} reflects the crack propagation period of the crack, with depth from a_H to a_f=B/2 in the untreated material. Thus, these values are the same as in Table 7a). The values of g and N_{eH} are given in Table 7b).

An attempt was made to obtain correlations of g with both nominal stress and strain reduction at weld toe, but these were not satisfactory. A reasonable correlation was, however, obtained with the depth of the crack, a_H, subjected to hammer peening, and this plot is shown in Fig. 13.

The results show that the gains due to repair by hammer peening of a cracked joint range from a factor of 1.0 to about II times the expected life of the joint, in case it was not repaired at all. The results indicate that higher benefits can be obtained with small repaired cracks.

For initial hammer peened joints, the rehabilitation treatment by hammer peening did not give any significant benefit, as shown in Fig. 14 in the S-N curves, where the results for the repaired joints are very close to the mean curve of the fatigue lives of the original specimens without repair (Figs 11 and 12). This is mainly due to the reduced effect of the compressive residual stresses in the repaired cracks that are still within the compressive stress field of the first initial treatment. The data for the three specimens tested under these conditions are given in Table 8.

TABLE 8 – VALUES OF FATIGUE LIFE FOR THE HAMMER PEENED JOINT REPAIRED BY HAMMER PEENING. $\Delta\sigma$=400MPa.

Specimen	a_H (mm)	c_H (mm)	N_{bH}	N_{Te}
38	2.37	5.75	53237	111939
46	3.98	16.05	124513	144252
47	2.865	10.9	59873	93809

3.5 RESIDUAL STRESS MEASUREMENTS

Values of the residual stresses were obtained in some selected specimens by the strain gauge hole drilling technique at the weld toe and in zones located at distances 2 and 5mm from the weld toe in the longitudinal x direction. The residual stresses were obtained for different types of specimens (as welded) not tested, hammer peened before testing and as welded, and after a fatigue test. The objectives of these tests were to quantify the residual stresses introduced by the hammer peening process, and to verify whether the fatigue loading changes the residual stress pattern in the as welded joints.

The results (Table 9) have shown that the residual stresses in the x direction are usually significantly higher than in the transverse z direction. This effect is predicted in the theory of welding. Both in the x and z directions, the residual stresses in the hammer peening condition are above those of the as welded condition. The maximum value of residual stresses are compressive, and occur in the location at the weld toe and in the longitudinal x direction.

Since the residual stress is of yield magnitude, when in compression its effect is beneficial for the fatigue behaviour of the joint, thus explaining the large increase in fatigue strength obtained for the hammer peened joints. The results also show that the effect of hammer peening, in terms of residual stresses, is localised near the weld toe where the treatment is applied since, at the zone 5mm away for the weld toe x=5mm, the residual stresses are negligible (Table 9).

The residual stresses in the as welded and after fatigue specimens are also low, at least 5mm away from the weld toe. Some relaxation effect of stresses may occur in the fatigue tested specimens, since both residual stresses in the x and z directions were found to be only slightly compressive, while the residual stresses in the as welded not fatigue tested specimens gave tensile values of low magnitude.

TABLE 9 – VALUES OF RESIDUAL STRESSES AT SURFACE (y≅0). 3PB SPECIMENS. NON-LOAD CARRYING JOINTS. St 52-3 GRADE STEEL.

	σ_x [MPa]			σ_z [MPa]		
Condition and technique	**Weld toe (x≅0)**	**X=2mm**	**X=5mm**	**Weld toe (x≅0)**	**X=2mm**	**X=5mm**
As welded not tested – Hole drilling	-90.7*	-18	91	-25.7*	11	66
Hammer peened not tested – Hole drilling	-486*	-286	14	-203.3	-142	-50
Fatigue tested – Hole drilling	-	-	-7	-	-	-33
As welded not tested – X-ray diffraction	-189	-138	-86	-78	-22	22
Hammer peened not tested – X-ray diffraction	-302	-258	-192*	-385	-171	150*

* Obtained by linear extrapolation.

TABLE 10 – DETAILS OF THE FE MESHES

	Number of nodes	**Number of elements**	**Degrees of freedom**
Rigid tool	1512	473	3024
Deformed tool	1704	529	3408

Close to the weld toe, the residual stress values obtained by hole drilling were below the values obtained by X-ray diffraction (Table 9). Although additional data is needed to draw more definitive conclusions, it is possible that this trend is partly attributed to the fact that, in the X-ray diffraction method, residual stresses are measured at the surface while, in the hole drilling method, these stresses represent an average of the stress distribution along the thickness of the layer of material subjected to measurement (in this case, the depth of the layer was about 2mm). Hence, the residual stresses obtained by hole drilling are not at the surface, but refer to a zone where $0<y<2$mm, where the residual stresses are expected to be lower than at the surface.

Using the elastic-plastic cycling constitutive equation of the material in compression (Table 2), the residual stresses σ_z and σ_x induced in hammer peening were computed with the 2FE program ABAQUS. Two options were assumed, as shown in Fig. 15. In the first type of simulation, a rigid (non-deformable) tool was considered (Fig. 15a)) and, in the second type of analysis, the stiffness of the tool was taken into account (Fig. 15b)) with the value of $E=2.1\times10^5$ MPa for the material of the tool. This value of E was measured with strain gauges bonded at the tool and applying a compressive load. Note that the measured value of E is the expected value for the material of the hammer peening tool (Fig. 2).

The details of the FE mesh for both cases are given in Table 10. The element type was the isoparametric contact with light nodes (CPE8). The geometry of the deformed meshes is also shown in Fig. 15 in the contact zone of the tool with the weld toe radius. It is seen that, to get the same level of accuracy in the stress results, additional nodes, elements and degrees of freedom are required in the analysis of the deformed tool (Table 10). The residual stress results were obtained for a single load application , with a static indentation with the value of the mean impact force given in Fig. 4, and representative of the hammer peening process. The radius of curvature at the wed toe was the mean value obtained, as referred in 2.2, and the radius of the spherical tool tip was 4.25mm. The depth of the indentation of the tool was taken as 0.015mm in the vertical direction. This was the vertical displacement (υ_y=0.015mm) used for the spherical surface of the tool for the static load of 1359N (Fig. 4), as perpetrates the surface of the material. This value of υ_y was assumed on the basis that, for this analysis, the hammer peening tool behaves similarly as the steel ball of the indenter of the Brinnell hardness tester acting on a plane surface tangent to the radius of curvature at the weld and in a direction 45° with this surface (Fig. 15). Using this model (25), with the equivalent Brinnell hardness value of the St 52-3 steel, before hammer peening (Fig. 5a)), the starting value of 0.015mm for the depth of indentation was found.

Using the approach referred above, the plots of the stresses are shown in Fig. 16 for the rigid tool (Fig. 15a)) and, in Fig. 17, for the deformed tool (Fig. 15b)). These stresses will be residual stresses induced in the material by the hammer peening, provided there is no stress relaxation.

The computed results show that the residual stresses are compressive and their value in compression decreases as the distances y (in the plate thickness) and x (longitudinal direction) increase from the weld toe. For the rigid tool case, the stress distributions σ_x and σ_z are close, and there are great variations as against the experimental results in Table 9.

The results for the deformed tool case (Fig. 17) gave stress values lower than the rigid tool case (Fig. 16). The stress distribution σ_{zz} (Fig. 17a)) is also close to the σ_{xx} one (Fig. 17b)), and there is a better agreement with the experimental results. Some stress relaxation may occur, since the experimentally measured residual stresses (Figs. 16 and 17), which will not show any significant variation with the time, were found in all cases, with values below the computed values obtained with a single load application at time $\cong$0. The differences between the experimental and computed values are in the range 10-20%. For both stresses, the depth of the zone, measured from the surface where the stress values are compressive at the weld toe, extends to a depth close to 2.5mm (Fig. 17).

CONCLUSIONS

- Fatigue strength has increased by a factor of 1.30 when the weld toe of 3PB, T non loading carrying joints of St 52-3 carbon steel was treated by hammer peening.
- The hardness distributions and the microhardness results have also shown that the depth of the zone affected by hammer peening is about 2.5mm, i.e. the material has hardened up to this depth. This was found to be the limit of the residual stress field created by the hammer peening.
- The effect of hammer peening to repair or rehabilitate an as welded joint with fatigue crack of known depth was detailed, and equations were derived to quantify this effect. A fatigue life improvement factor, g, was defined for rehabilitation of joints by hammer peening. This factor was found to be dependent on the repair crack depth, increasing as the initial crack depth decreases, i.e. the treatment is more effective for cracks with depths below 2mm, where the fatigue life of the repaired joint has increased by about one order of magnitude (g$\cong$10).
- For joints that were subjected, initially, to an hammer peening treatment to increase their fatigue life in service, subsequent repair of fatigue cracks by hammer peening did not give any significant increase in fatigue life as happens with those without the repair.
- The residual stresses induced by hammer peening at the weld toe were found to be greater along longitudinal direction of the plate than along the transverse direction. The peak residual stresses near the weld toe were found to be of yield magnitude in compression, justifying the great beneficial benefit of hammer peening.
- Good agreement was found between the computed residual stress values resulting from hammer peening and obtained by an elastic-plastic 2DFE program, and the experimental values obtained at the surface by X-ray diffraction near the surface by hole drilling.

REFERENCES

(1) Branco, C.M., Dickerson, T., Final report of ECSC/EEC project "Weld Improvement Methods for Low Cycle Fatigue Applications", Contract Nr. 7210-MC/931, CEMUL/IST, July 94 (in cooperation with TWI, UK, under contract ECSC 7210-MC/801).

(2) Branco, C.M., Gomes, E.C., "Development of Fatigue Design Curves for Weld Improved Joints", Proc. Int. Conf. Fatigue Design 95, FD95, Helsinki, Finland, Vol. III, pp. 9-21, 1995.

(3) Maddox, S.J., "Fatigue Strength of Welded Structures", Ed. Abington Publishing, Cambridge, UK, 1991.

(4) Branco, C.M., Fernandes, A.A., Castro, P.T., "Fatigue of Welded Structures" (in Portuguese), Cap. 11, Ed. Calouste Gulbenkian Foundation, Lisbon, 1999.

(5) Booth, G.S. (ed.), "Improving the Fatigue Performance of Welded Joints", The Welding Institute, Cambridge, UK, 1999.

(6) Offshore Installations; Guidance on Design, Construction and Certification, UK Department of Energy, HMSO, Fourth Edition, 1990.

(7) "British Standard Specifications for Unfired Fusion Welded Pressure Vessels", BS5500, 1990, British Standards Institution, London, UK.

(8) Haagensen, P.J., Slind, T., "Weld Improvement Methods and Fatigue Design Rules", Proc. Int. Conf. Fatigue and Welded Constructions, The Welding Institute, UK, 1987.

(9) Huther, I, Lieurade, H.P., Sonissi, R., Nussbaumer, A., Chabrolin, B., Janosh, J.J., "Analysis of Results on Improved Welded Joints", Welding in the World, 37, 5, pp. 242-266, 1996.

(10) Maddox, S.J., "The Application of Fatigue Life Improvement Techniques to Steel Welds", IIW Commission XIII Workshop on Improvement Methods, International Institute of Welding, Proc. 51st Annual Assembly, Hamburg, Germany, September 1998.

(11) Haagensen, P.J., Maddox, S.J., "Specifications for Weld Toe Improvement by Burr Grinding, TIG Dressing and Hammer Peening for Transverse Welds", IIW Document, Commission XIII, Working Group 2, WG2, International Institute of Welding, 1995.

(12) Fisher, J.W., Dexter, R.J., "Weld Improvement for Fatigue Life Extension", Proc. Int. Conf. Fatigue, Toronto, Canada, 9-10 May 1994, publ. AWS, pp. 82-87, 1994.

(13) Fisher, J.W., Dexter, R.J., "Field Experience with Repair of Fatigue Cracks", Proc. Int. Conf. Fatigue, Toronto, Canada, 9-10 May 1994, publ. AWS, pp. 82-87, 1994.

(14) Miki, C., "Repairing and Reinforcing of Fatigue Damaged Steel Bridges", Proc. Int. Conf. On Performance of Dynamically Loaded Welded Structures, IIW 50th Annual Assembly Conference, San Francisco, USA, July 1997, publ. Welding Research Council, pp. 286-298, 1997.

(15) Jarurai, K., Farras, J., Haagensen, P.J., "The Effect of Post-Welding Treatments on the Optimum Fatigue Design of welded I-Beams", IIW Meeting, Lisbon, 1999, Paper XV, 1025-99, and XIII, 1775-99.

(16) Branco, C.M., Infante, V., Maddox, S.J., "A Fatigue Study on the rehabilitation of welded Joints", Proc. Meeting of the International Institute of Welding, IIW, Lisbon, 17-24 July 1999, Commission XIII, Paper XIII-1769-99.
(17) Eurocode 3: "Design of Steel Structures", Part 1, general rules for buildings, Commission of the European Communities, 1990.
(18) Hobbacher, A. (Ed.), "Fatigue Design of welded Joints and Components", International Institute of Welding, IIW, Abington Publishing, Cambridge, UK, 1996.
(19) Branco, C.M., Maddox, S.J., Infante, V., Gomes, E.C., "Fatigue Performance of TIG and Plasma Welds in Thin Sections", Int. J. Fat., 22, 6, pp. 589-602, 1999.
(20) Ferreira, J.M., Pereira, A.H., Branco, C.M., "A Fracture Mechanics Based Fatigue Life Prediction for Welded Joints of Square Tubes", Thin Walled Structures, 21, 1995, pp. 107-120.
(21) Martins, R.F., "Application of Probabilistic Fracture Mechanics of Fatigue of Welded Structures" (in Portuguese), MSc Thesis, Technical University of Lisbon, IST, April 1999.
(22) Ferreira, J.M., Branco, C.M., "Fatigue Life Predictions in Welded Joints Using 2D and 3D K Solutions", Fat. Fract. Eng. Mat. Struct., 16, 3, pp. 303-313, 1993.
(23) British Standards Institution, "Guidance on Methods for the Acceptance of Flaws in Structures", PD6493, Proposal BS7910, 1999, UK.
(24) Hobbacher, A., "Fatigue design of welded joints and components", IIW publication, Abington Publishing, UK, 1996.
(25) DIN 50351, "Brinell hardness test for metallic materials", 1996.

ACKNOWLEDGEMENTS

The specimens were kindly supplied by The Welding Institute (TWI), Cambridge, UK. The authors express their gratitude for the support and useful discussions with Dr. S. Maddox, of TWI.

LIST OF FIGURES

Fig. 10 – Plots of variation of local strain at the weld toe in the fatigue crack zone, as a function of number of elapsed cycles. T joints. Bending. R=0.1. St 52-3 steel.

a) As welded, with fatigue marking at 40% strain reduction, of a crack depth of 3.862 mm. $\Delta\sigma$=325 MPa.

b) As welded, repaired by hammer peening of a crack depth of 3.3 mm. Fatigue marking at 15% strain increase. $\Delta\sigma$=300 MPa.

Fig. 11 – S-N curves of the as welded, hammer peened and ground joints. 3PB T non-load carrying joints. St 52-3 steel.

Fig. 12 – S-N data for the repaired joints by hammer peening. 3PB T non-load carrying joints. Medium strength St 52-3 steel.

Fig. 13 – Gain factor, g, in fatigue life due to hammer peening treatment against depth of the crack repaired by hammer peening. 3PB T non-load carrying joints. St 52-3 steel.

Fig. 14 – S-N data for the hammer peened joints repaired by hammer peening. 3PB T non-load carrying joints. St 52-3 steel.

Fig. 15 – FE mesh and geometry of the hammer peening tool to calculate the stress distributions induced by hammer peening process.

a) Rigid tool.

b) Deformed tool. E = 2.1 x 10^5 MPa.

Fig. 16 – Residual stress distributions along the fatigue crack growth y direction, introduced by hammer peening process. Rigid hammer peening tool. Experimental results of Table 9.

a) Z direction. σ_{zz}.

b) X direction. σ_{xx}.

Fig. 17 – Residual stress distributions along the fatigue crack growth y direction, introduced by hammer peening process. Deformed hammer peening tool. Experimental results of Table 9.

a) Z direction. σ_{zz}.

b) X direction. σ_{xx}.

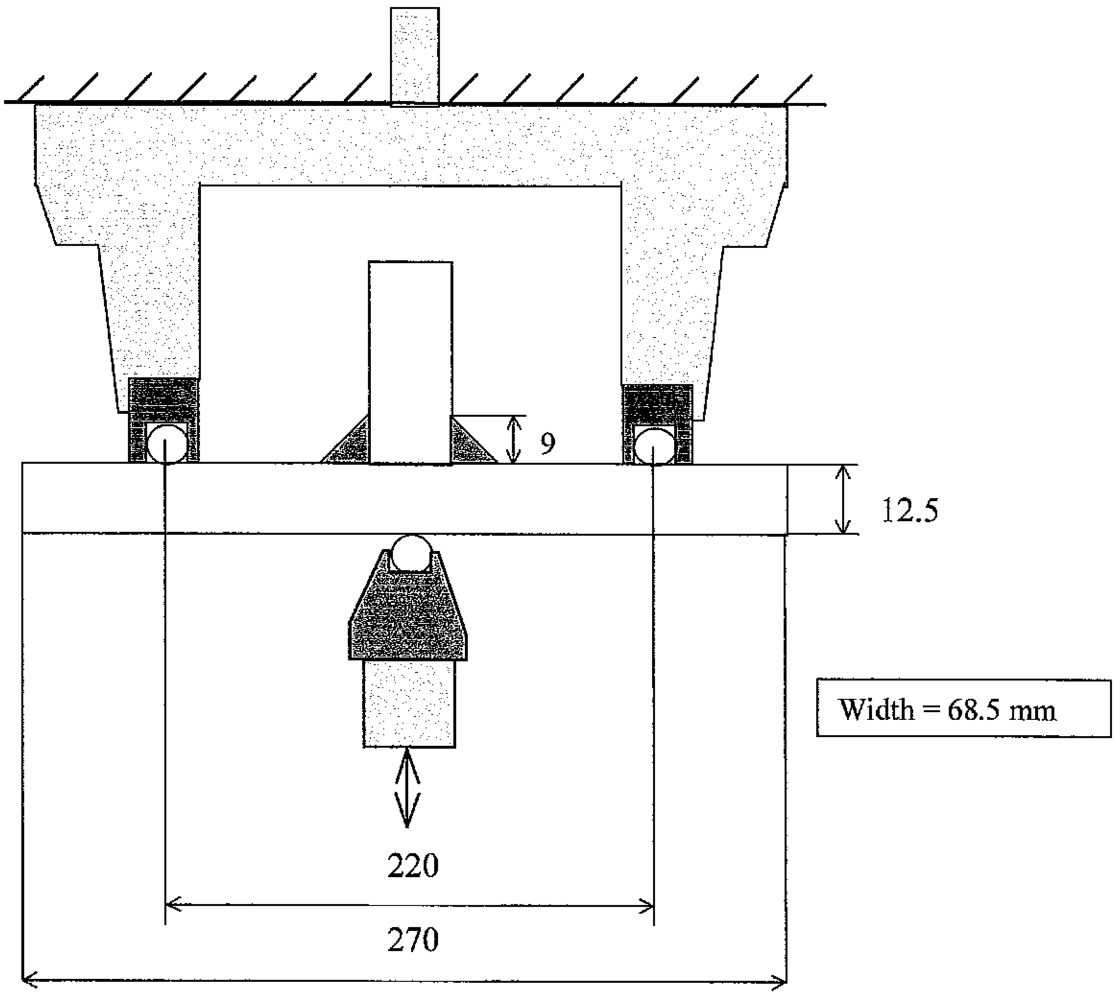

Fig. 1 – Schematic set-up for the 3PB fatigue tests in the welded joints. R=0.1. Medium strength carbon steel St 52-3.

Fig. 2 - Hammer peening tool with strain gauges to measure the impact force and energy. Material: Low alloy forget heat treated medium carbon steel with C – 0.41; Mn – 0.75; Si – 0.23; Cr – 1.1; Mo – 0.18; V – 0.035; W – 0.1.

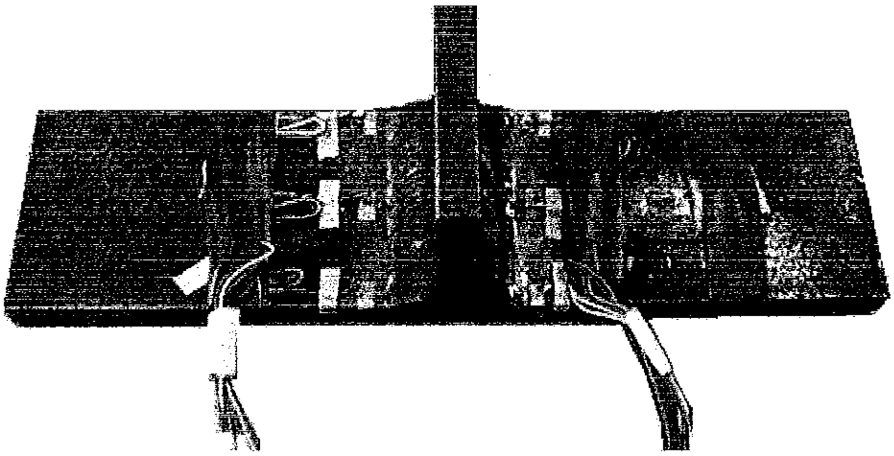

Fig. 3 – Set-up of the strain gauges used to monitor the onset of crack initiation and detect cracking.

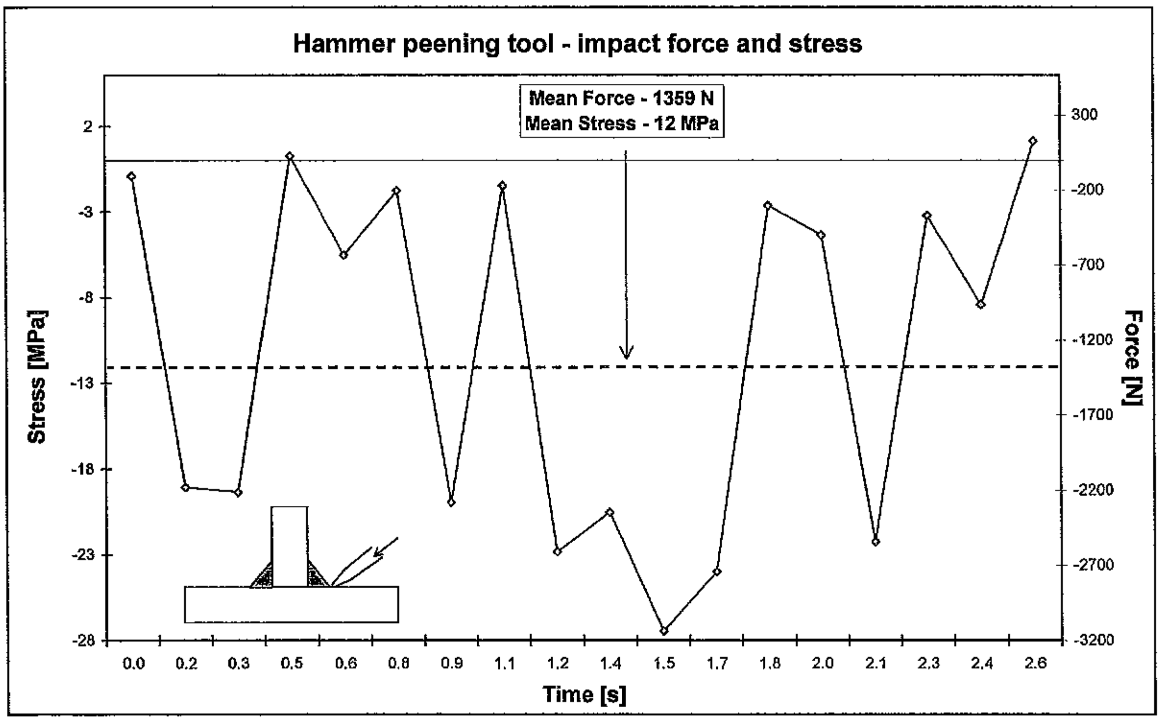

Fig. 4 – Variation of impact force and impact stress measured in the hammer peening tool during the treatment at the weld toe.

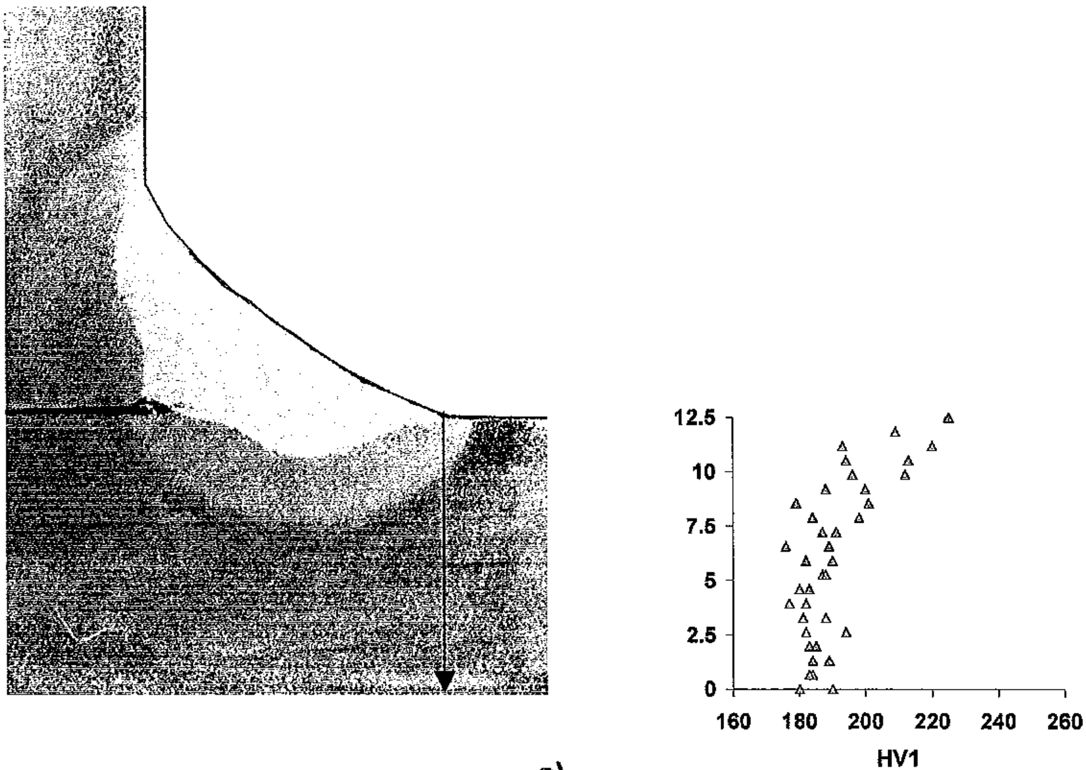

a)

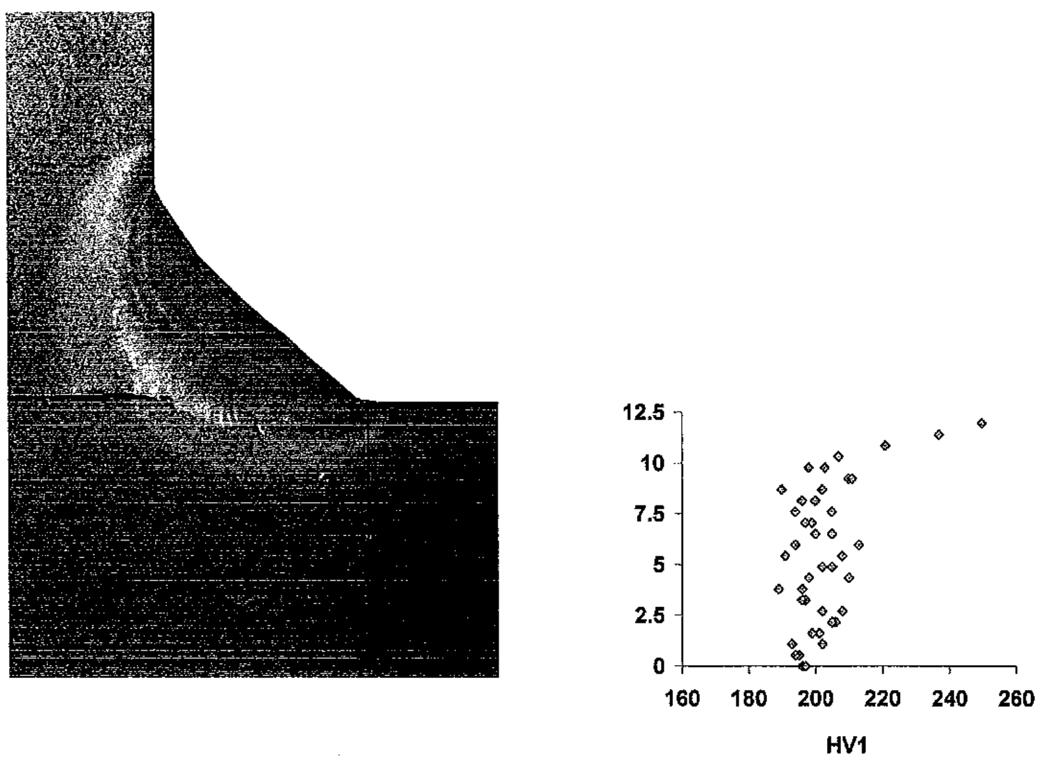

b)

Fig. 5 – Hardness profiles in the welded joints. **a)** As welded, HV1. **b)** Hammer peened, HV1. Steel St 52-3.

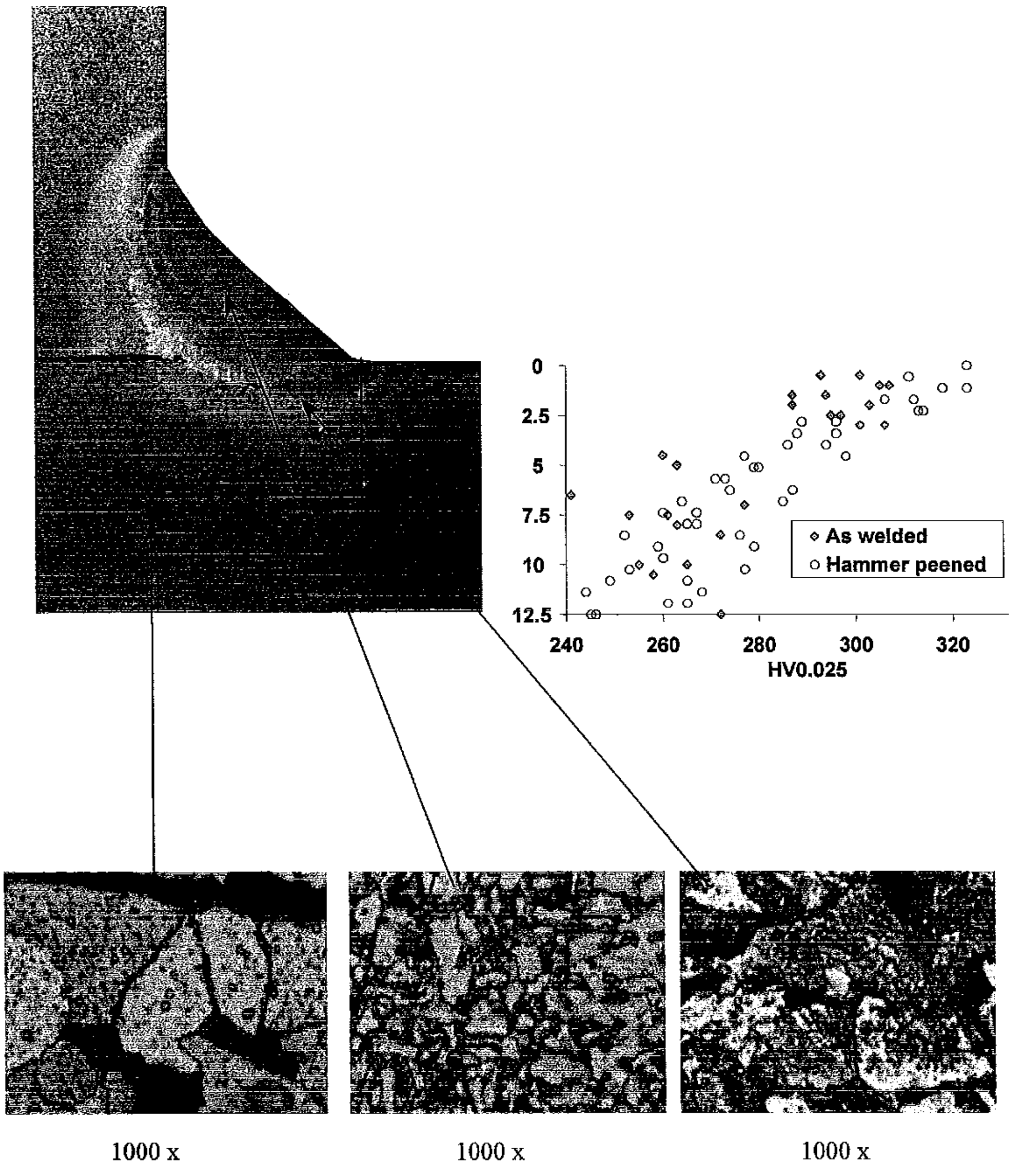

Fig. 6 – Hardness profiles in the welded joints. As welded and hammer peened, microhardness, 25 gf. Microstructure of base metal, weld metal and HAZ. Amp. 1000x

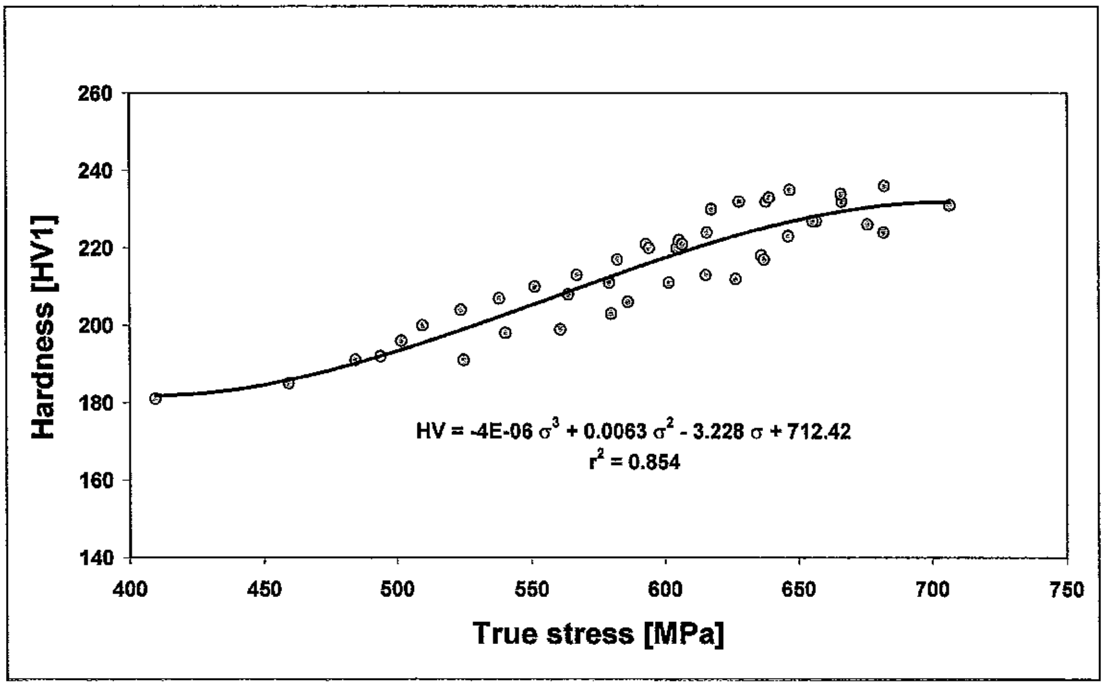

a)

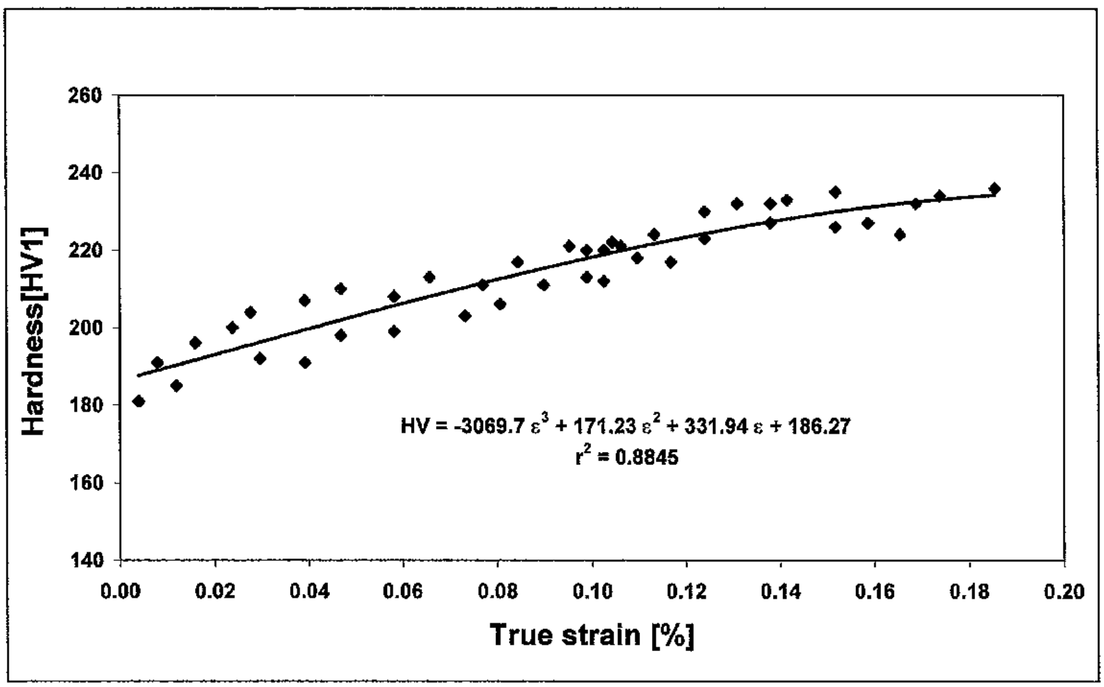

b)

Fig. 7 – Derivation of true-stress, true strain curve from hardness measurements.
Steel 52-3.

a) Hardness HV1 *versus* true stress.

b) Hardness HV1 *versus* true strain.

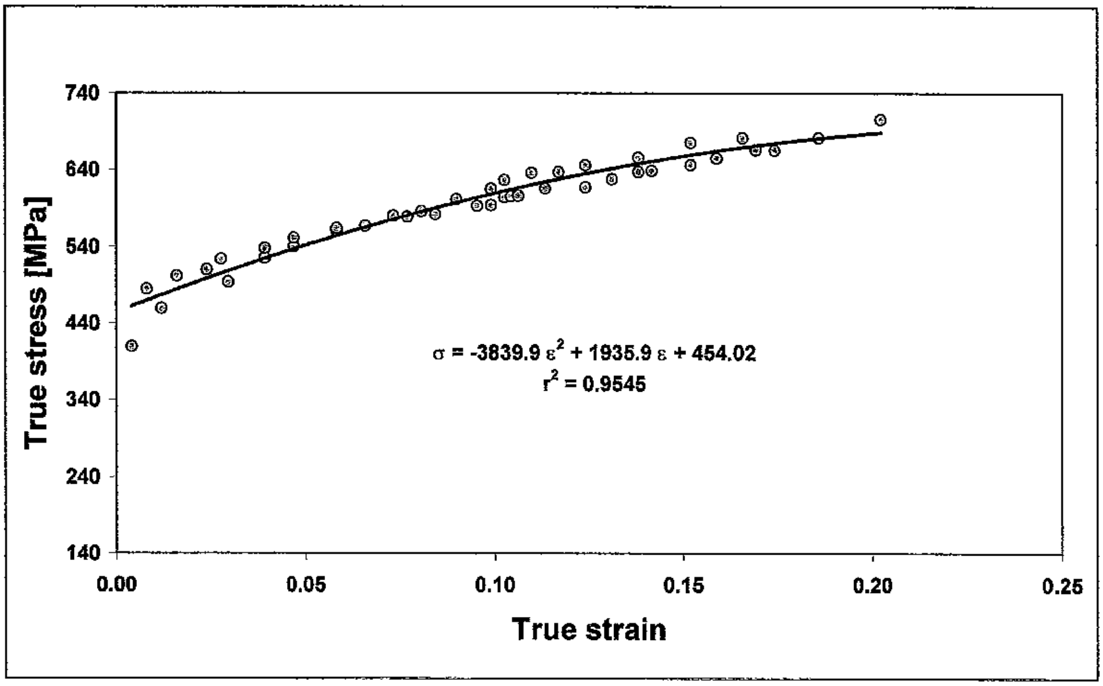

c)

Fig. 7 – Derivation of true-stress, true strain curve from hardness measurements. Steel 52-3.

c) True stress-true strain curve.

a) As welded only with fatigue marking at 40% strain reduction, of a crack depth of 3.862 mm. Specimen 23. $\Delta\sigma$=325 MPa. N_r= 489201 cycles.

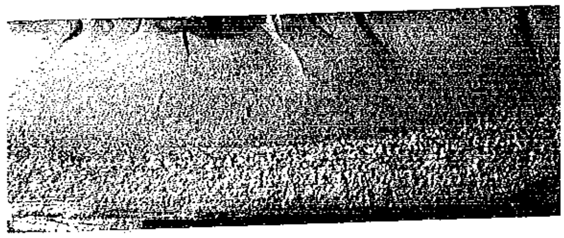

b) As welded, repaired by hammer peening of a crack depth of 1.27 mm. Specimen 57. Fatigue marking at 25% strain reduction. $\Delta\sigma$=325 MPa. N_r= 900266 cycles.

c) Hammer peened after welding and repaired by hammer peening of a crack depth of 3.98 mm. Specimen 46. Fatigue marking at 15% strain increase. $\Delta\sigma$=500 MPa. N_r=144252 cycles.

Fig. 8 – Macros of fracture surfaces of fatigue specimens. T joints. Bending. R=0.1. St 52-3 steel.

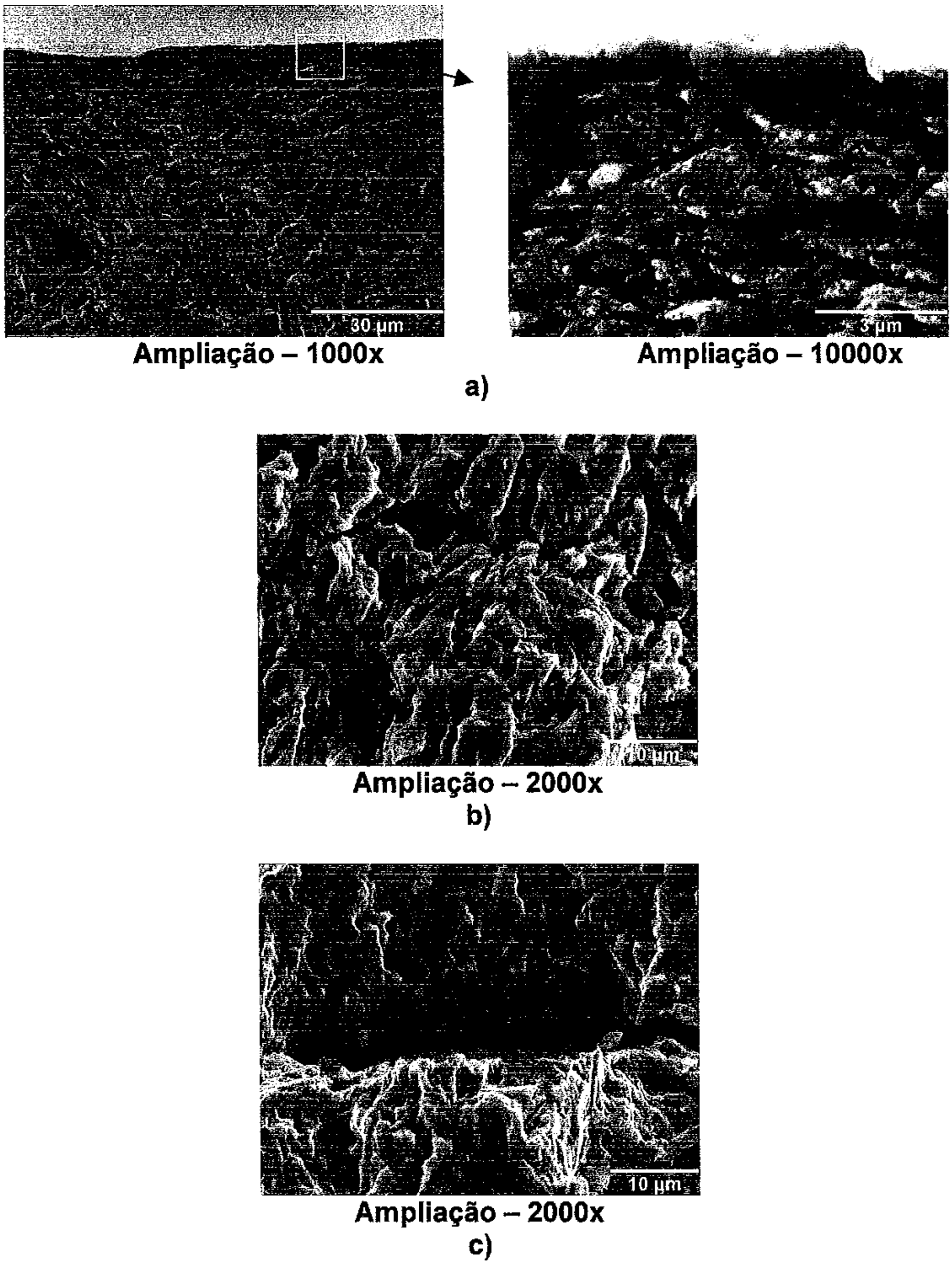

Fig. 9 – SEM fracture surfaces. Steel St 52-3.
a) Hammer peened after welding. Specimen 41. $\Delta\sigma$ = 400 MPa.
b) As welded, repaired by hammer peening of a crack depth of 1.441 mm. Specimen 53. $\Delta\sigma$ = 400 MPa.
c) As welded, repaired by hammer peening of a crack depth of 4 mm. Specimen 28. $\Delta\sigma$ = 400 MPa.

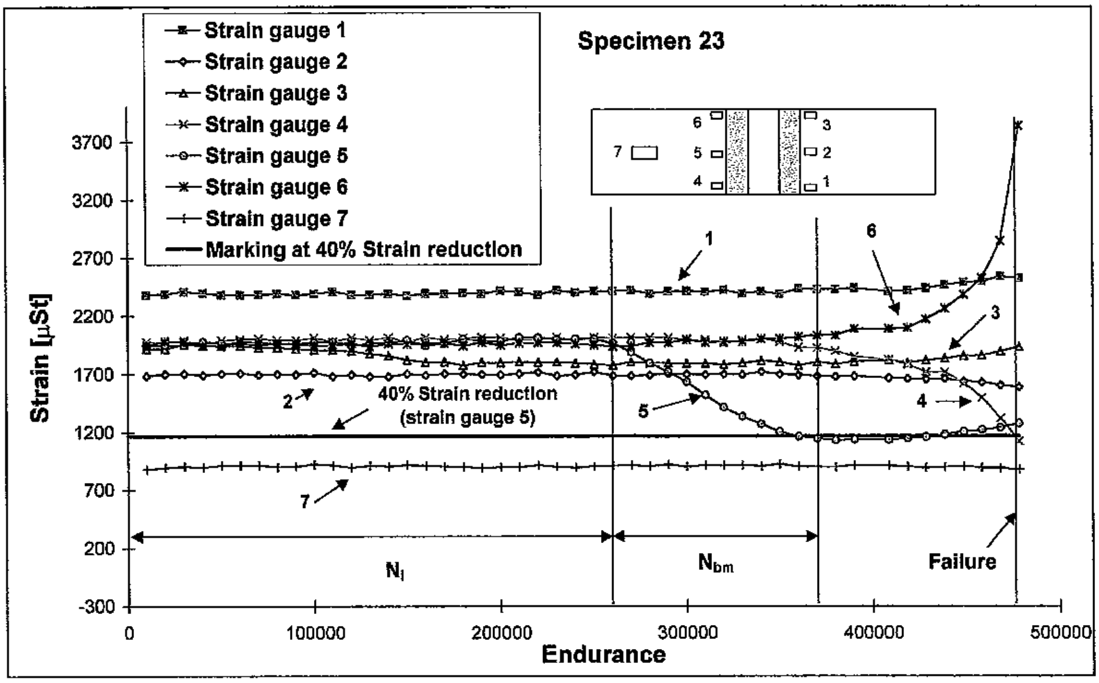

a) As welded, with fatigue marking at 40% strain reduction, of a crack depth of 3.862 mm. $\Delta\sigma$=325 MPa.

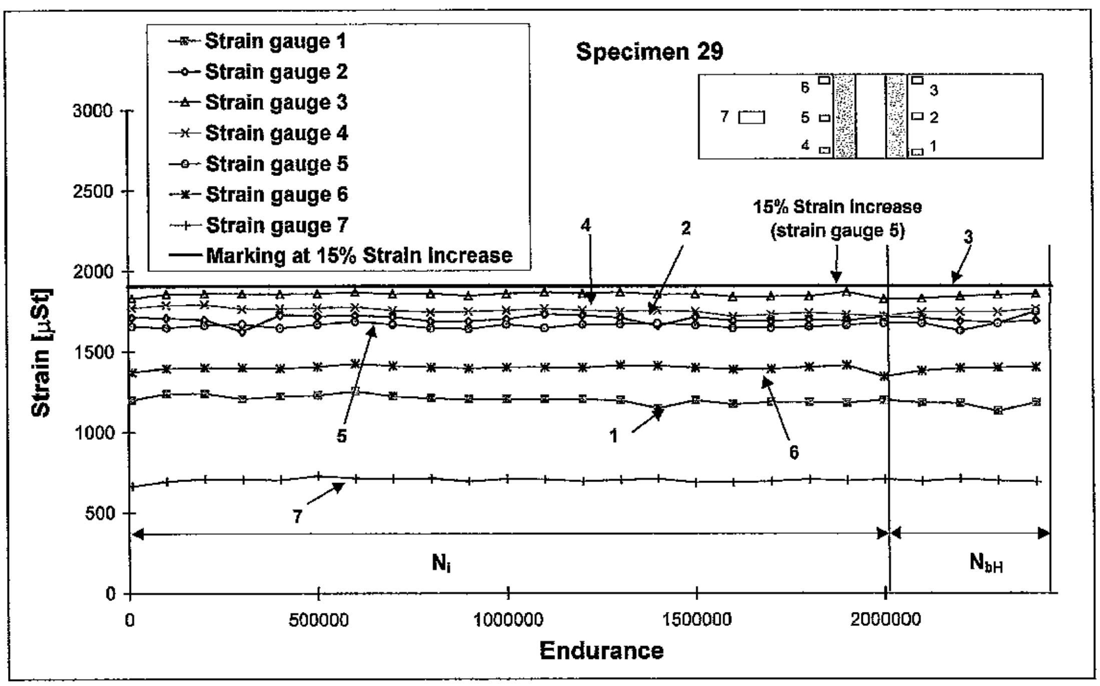

b) As welded, repaired by hammer peening of a crack depth of 3.3 mm. Fatigue marking at 15% strain increase. $\Delta\sigma$=300 MPa.

Fig. 10 – Plots of variation of local strain at the weld toe in the fatigue crack zone, as a function of number of elapsed cycles. T joints. Bending. R=0.1. St 52-3 steel.

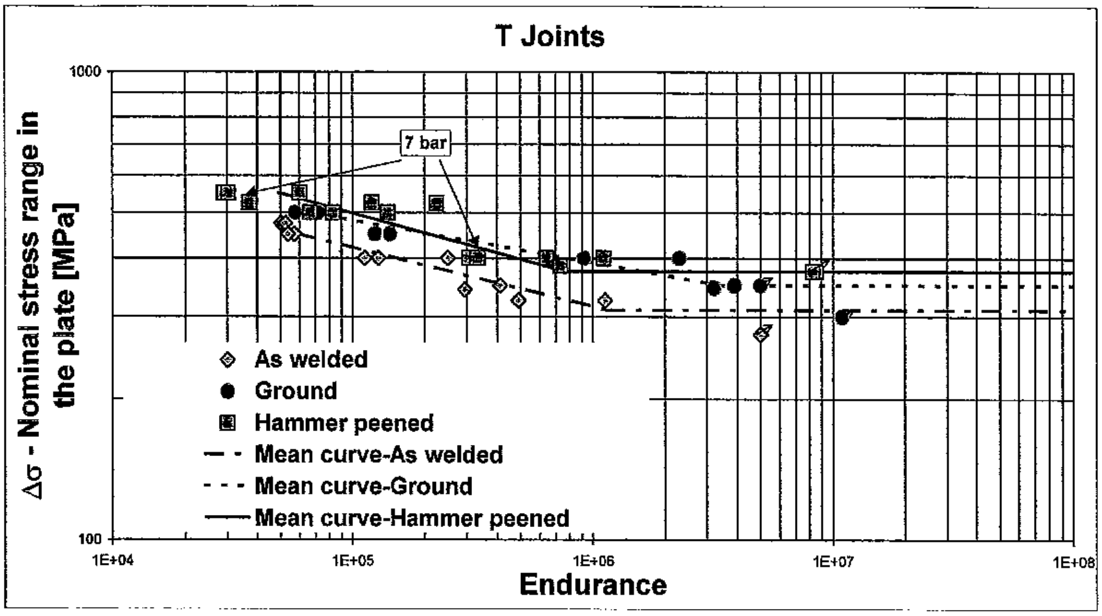

Fig. 11 – S-N curves of the as welded, hammer peened and ground joints. 3PB T non-load carrying joints. St 52-3 steel.

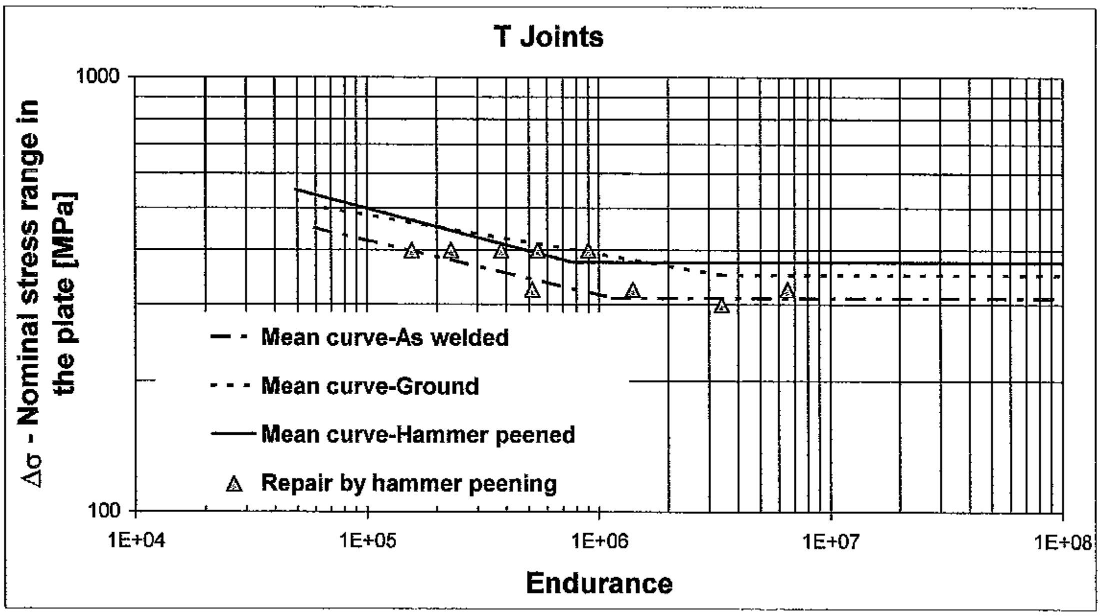

Fig. 12 – S-N data for the repaired joints by hammer peening. 3PB T non-load carrying joints. Medium strength St 52-3 steel.

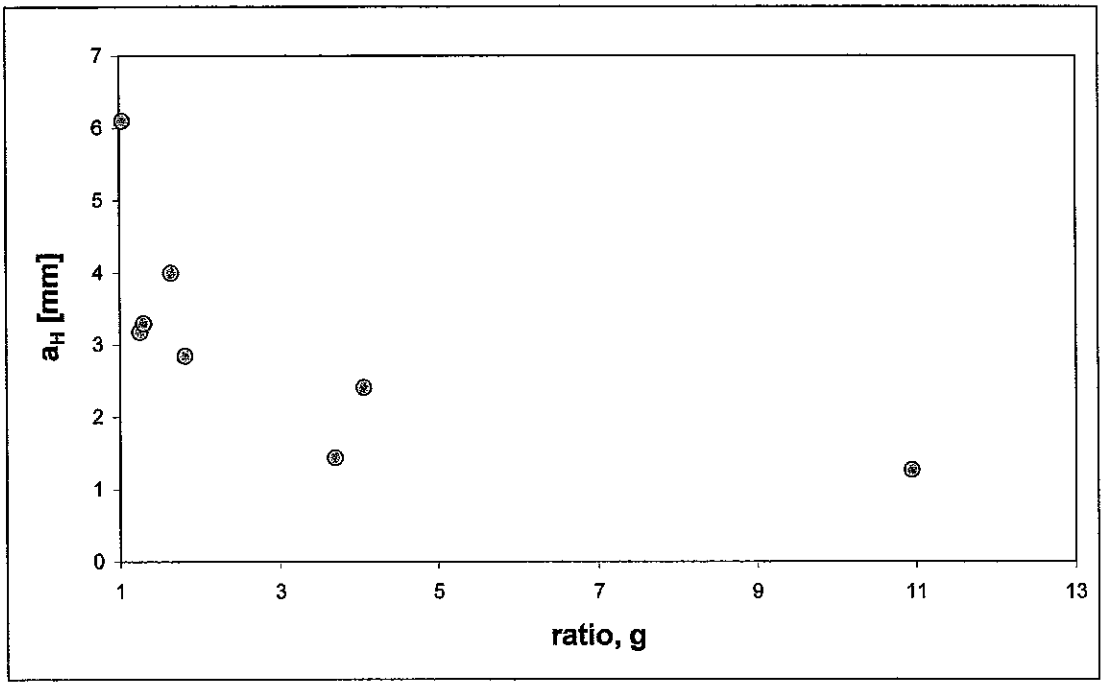

Fig. 13 – Gain factor, g, in fatigue life due to hammer peening treatment against depth of the crack repaired by hammer peening. 3PB T non-load carrying joints. St 52-3 steel.

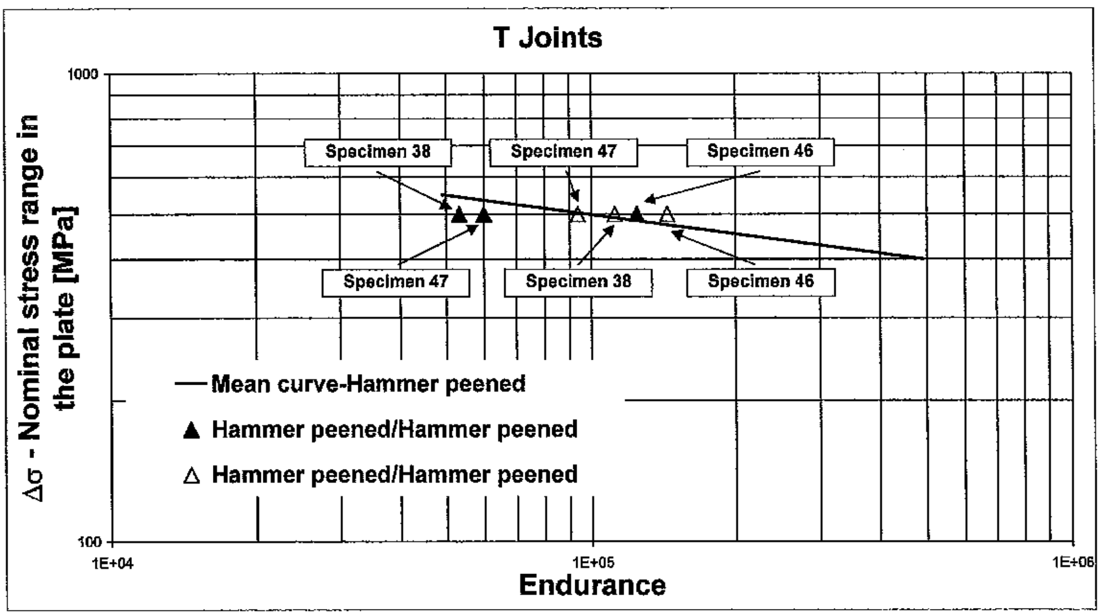

Fig. 14 – S-N data for the hammer peened joints repaired by hammer peening. 3PB T non-load carrying joints. St 52-3 steel.

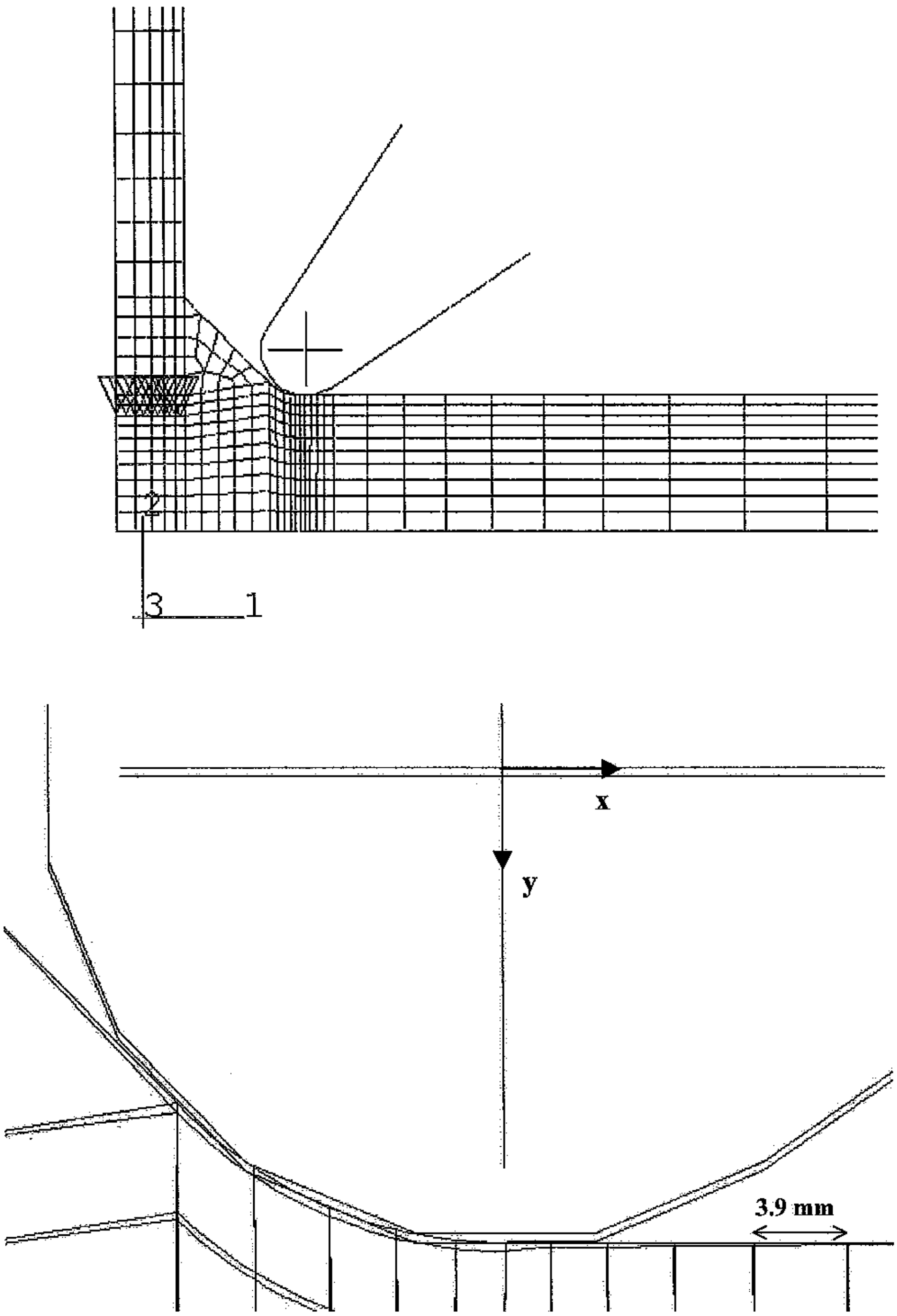

a)

Fig. 15 – FE mesh and geometry of the hammer peening tool to calculate the stress distributions induced by hammer peening process.
a) Rigid tool.

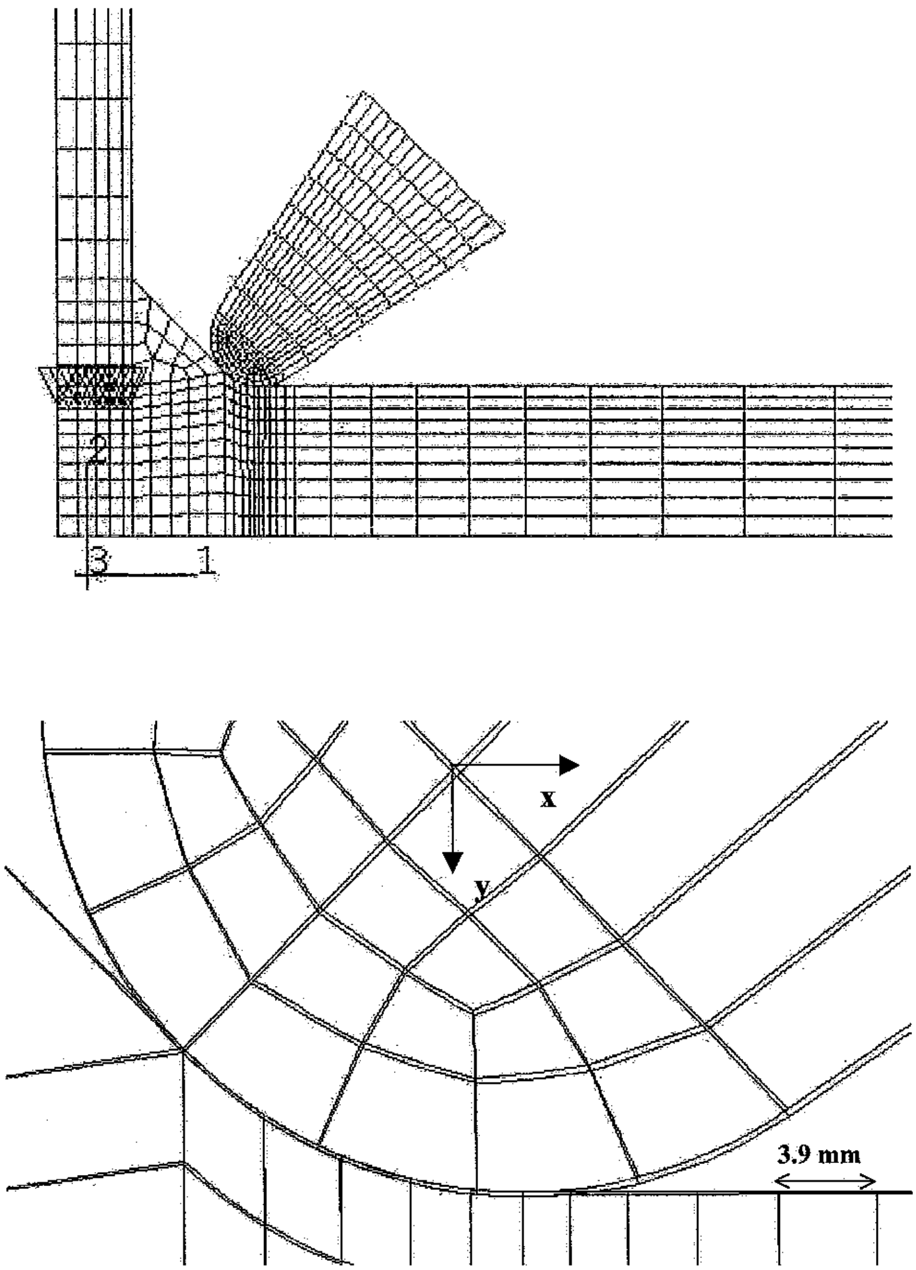

b)

Fig. 15 – FE mesh and geometry of the hammer peening tool to calculate the stress distributions induced by hammer peening process.
b) Deformed tool. E = 2.1 x 10^5 MPa.

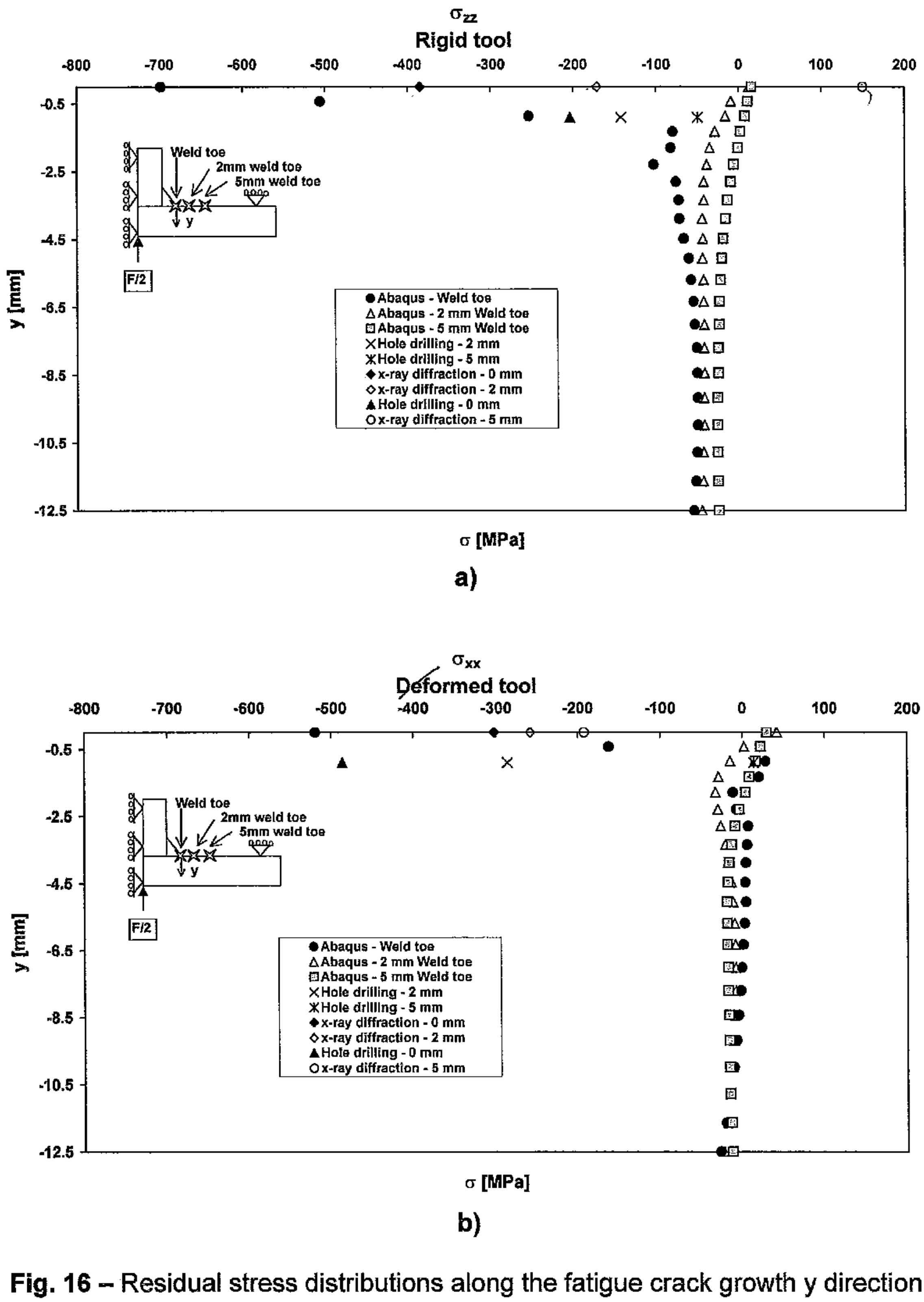

Fig. 16 – Residual stress distributions along the fatigue crack growth y direction, introduced by hammer peening process. Rigid hammer peening tool. Experimental results of Table 9.

a) Z direction. σ_{zz}.

b) X direction. σ_{xx}.

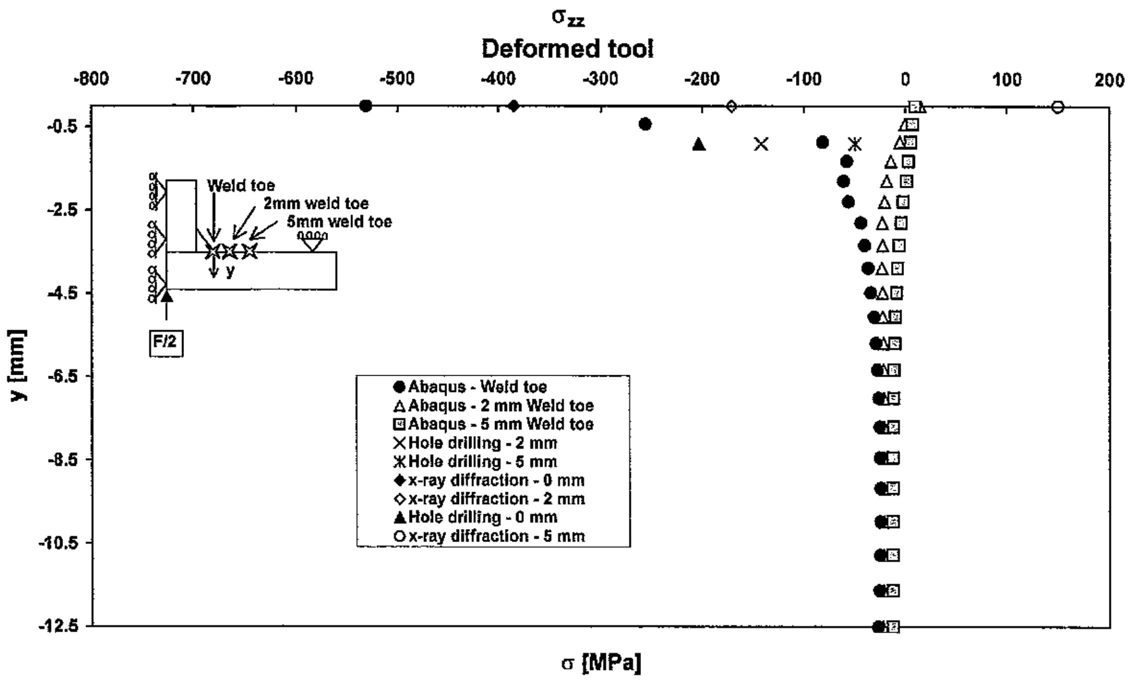

a)

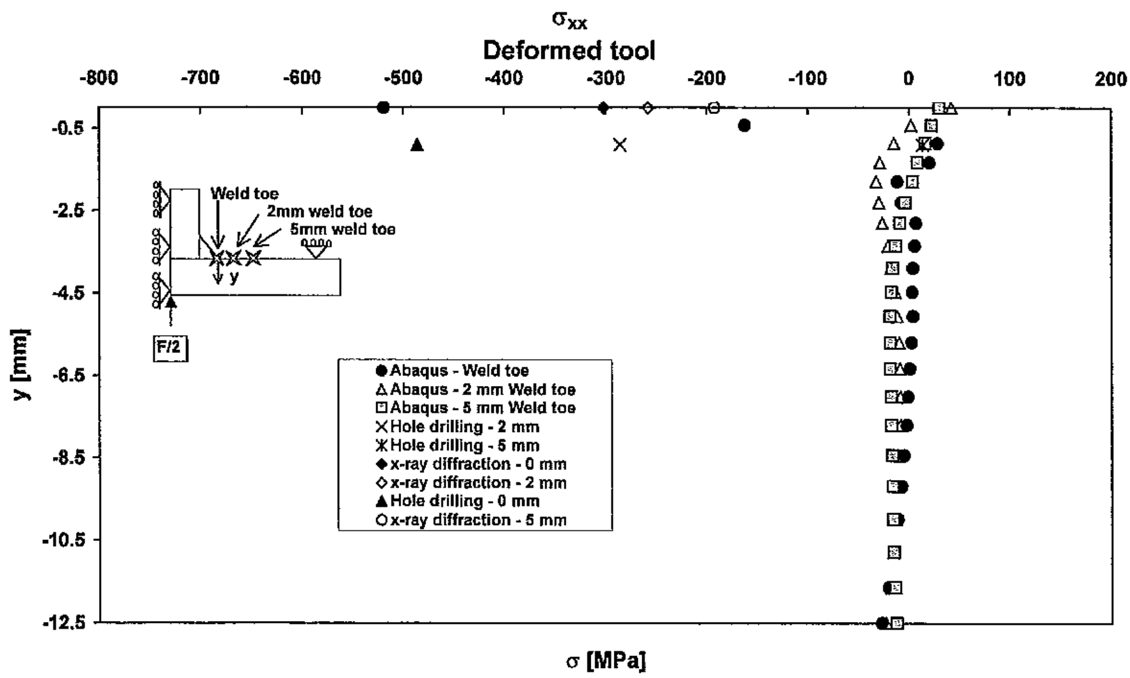

b)

Fig. 17 – Residual stress distributions along the fatigue crack growth y direction, introduced by hammer peening process. Deformed hammer peening tool. Experimental results of Table 9.

a) Z direction. σ_{zz}.

b) X direction. σ_{xx}.